

# Consequences of using a smooth cosmic distance in a lumpy universe. I.

Obinna Umeh<sup>✉\*</sup>

*Institute of Cosmology and Gravitation, University of Portsmouth,  
Portsmouth PO1 3FX, United Kingdom; Department of Physics,  
University of the Western Cape, Cape Town 7535, South Africa;  
and Department of Mathematics and Applied Mathematics, University of Cape Town,  
Rondebosch 7701, South Africa*



(Received 23 February 2022; accepted 5 July 2022; published 21 July 2022)

How do we appropriately fit a model based on an idealized Friedmann-Lemaître Robertson-Walker spacetime to observations made from a single location in a lumpy universe? We address this question for surveys that measure the imprints of the baryon acoustic oscillation in galaxy distribution and the peak apparent magnitude of the type 1A supernova. These observables are related to the cosmological model through the Alcock-Paczyński parameters and the distance-redshift relation. Using the corresponding inhomogeneous spacetime expressions of these as observed data, we perform a parameter inference assuming that the background Friedmann-Lemaître Robertson-Walker model is the correct model of the Universe. This process allows us to estimate the best fit Hubble rate and the deceleration parameter. We find that the inferred Hubble rate from the monopole of the Alcock-Paczyński parameters is in tension with the Hubble rate determined using the distance-redshift relation. The latter gives the best fit Hubble rate for the cosmological expansion. The constraint on the Hubble rate from the Alcock-Paczyński parameters is contaminated by the environment. When the environmental contribution is restricted to modes in the Hubble flow, we find about (9–12)% discrepancy in the Hubble rate. Finally, we comment on the insufficiency of the method of cosmography in constraining the deceleration parameter.

DOI: [10.1103/PhysRevD.106.023514](https://doi.org/10.1103/PhysRevD.106.023514)

## I. INTRODUCTION

The distribution of large scale structures in the Universe on ultralarge scales appear homogeneous and isotropic [1–3]. On scales of superclusters, there are inhomogeneities [4]. The Universe seen on scales of clusters appears very lumpy with sources moving with discernible peculiar velocities within clusters and clusters interacting gravitationally with each other [5,6]. Ellis and Stoeger pointed out in [7] that fitting models based on homogeneous and isotropic Friedmann-Lemaître Robertson-Walker (FLRW) spacetime to observation of a lumpy universe leads to a geometry that ignores on average the details present on small scales. Such a description of physical reality by the best-fit FLRW model embodies a smoothing scale that is usually not made explicit. Ellis and Stoeger further argued that any relevant averaging procedure that yields a best-fit FLRW model must be performed on the past light cone of the observer [7,8]. This is particularly important because averaging on the hypersurface of constant time could be gauge dependent. The question of which of the  $N$ -possible observers in the Universe sees a homogeneous and isotropic FLRW spacetime is still unaddressed [8,9]. It is

important to note that observing the isotropic distribution of matter on the past light cone of an observer does not immediately imply a homogeneous distribution of matter without a further assumption of the Copernican principle [10,11]. This work is about the cosmological fitting problem in the light of the current Hubble tension.

Hubble tension refers to the discrepancies in the value of the Hubble rate,  $H_0$ , when late/early time observations are interpreted using the FLRW spacetime. For example, the SH0ES collaboration constrains  $H_0$  to be  $H_0 = 73.2 \pm 1.3$  km/sec/Mpc from the intercept of the Hubble diagram of type 1A supernova (SNIa) with the absolute luminosity calibrated using nearby Cepheid variables [12], detached eclipsing binary system in the large magellanic cloud [13] and distance to the NGC 4258 [14]. The Carnegie-Chicago Hubble Program (CCHP) constrains  $H_0$  to be  $H_0 = 69.6 \pm 1.9$  km/sec/Mpc using the information contained in the Hubble diagram at low redshift. Here, the absolute luminosity is calibrated using the tip of the red giant branch (TRGB) stars in the Hertzsprung-Russell diagram [15]. The calibration of the absolute luminosity using different anchors by the two groups does not seem to be the source of the discrepancy but rather the ability to synchronize the zero-point of the distance modulus [16]. The baryon acoustic oscillation (BAO) spectroscopic survey, however, constrains a combination of the Alcock-Paczyński

\*obinna.umeh@port.ac.uk

parameters [17] with respect to the BAO peak at an effective redshift different from zero. The Alcock-Paczyński parameters are then interpreted in terms of the flat FLRW model to make a determination of  $H_0 = 68.6 \pm 1.1$  km/sec/Mpc [18–20]. There are a whole lot of other determinations of  $H_0$  with values falling into either within BAO or SHOES categories, for details see Ref. [21].

All these efforts assume that the FLRW spacetime provides the correct description of the Universe on all scales [12,15,18,20,22,23], yet they return different determinations of  $H_0$ . We study this tension by averaging over the spacetime independent inhomogeneous generalization of each of the observable-redshift relations used in the determination of  $H_0$ . We make use of the formalism developed by Kristian and Sachs [24] to derive these equations in the limit of small redshifts. We fit the FLRW model at fixed redshift to the corresponding monopole (past-light cone average) of the generalized observable-redshift relations. We made use of the  $1 + 3$  covariant decomposition formalism developed in [25,26] to decompose the observable-redshift relations into covariant irreducible units. In addition, we made use of the observer past-light cone moment decomposition formalism developed in [27,28] to extract the monopole in a coordinate independent way. This allows us to obtain the best-fit Hubble rate and the deceleration parameter,  $q_0$ , using each of the observable-redshift relations by matching the monopole of the arbitrary inhomogeneous model to that of the homogeneous and isotropic FLRW spacetime order by order in redshift.

We find that the difference between the Hubble rate obtained from fitting the local distance modulus for the SNIa and the Alcock-Paczyński parameters to the FLRW model is proportional to the square of the shear tensor associated with a geodesic observer in our local group. In a perturbed FLRW spacetime, this term is proportional to the variance in the mass density field fluctuation smoothed at scale  $R$ . We show that the smoothing scale  $R$  corresponds to a scale where the geometry of the local observer decouples from the large scale expansion of the Universe (i.e., the radius of the zero-velocity surface). We argue that the smoothing scale must be set to this value in order to avoid the caustics or the conjugate point at the boundary of our local group [29]. Taking the mass of our local group to be  $M_{\text{LG}} \sim (10^{11} - 10^{12}) M_{\odot}$  [30–32] gives a smoothing scale of  $R \sim (0.8 - 1.2)$  Mpc. This translates to about (9–12)% discrepancy in the Hubble rate and this is the amount needed to resolve the supernova absolute magnitude tension as well [33]. In addition, we find that the deceleration parameter  $q_0$  obtained from cosmography is also impacted by cosmic structures. We find a discrepancy in the determination of  $q_0$ . The value we find is in agreement with the recent measurement of  $q_0$  from Pantheon supernova sample [34]. It is important to note that monopole of the low redshift Taylor series expansion of the area distance differs significantly from the full expression [35], therefore, this result may not be trusted. We argue that it is rather an

indication of a breakdown of the low redshift Taylor series expansion since the determination using the full expression gives a much lower value [36].

The rest of the paper is organized as follows: we describe the underlying philosophy behind the cosmological fitting problem in Sec. II. This is followed by a description of the generalized spacetime independent inhomogeneous models for the area/luminosity distance in Sec. II A. We describe how to fit inhomogeneous models of various observables to the FLRW model in Sec. III. We specialized the discussion to a perturbed FLRW model in Sec. IV. We discuss the existence of a causal horizon and how to identify it in Sec. IV A. We conclude in Sec. V. We provide details on how the generalized inhomogeneous observable-redshift relations were derived in the Appendix.

*Cosmology.*—We adopt the following values for the cosmological parameters of the standard model [22]: the dimensionless Hubble parameter,  $h = 0.674$ , baryon density parameter,  $\Omega_b = 0.0493$ , dark matter density parameter,  $\Omega_{\text{cdm}} = 0.264$ , matter density parameter,  $\Omega_m = \Omega_{\text{cdm}} + \Omega_b$ , spectral index,  $n_s = 0.9608$ , and the amplitude of the primordial perturbation,  $A_s = 2.198 \times 10^{-9}$ .

## II. INTRODUCTION TO THE COSMOLOGICAL FITTING PROBLEM

There are two approaches for building a model of the Universe; the pragmatic and observational approaches. The pragmatic approach makes assumptions about the geometry of the Universe and then use observations to validate those assumptions. For example, the standard model of cosmology is built on *a priori* assumption that all physical quantities measured by a comoving observer are spatially homogeneous and isotropic (cosmological principle). This assumption restricts a set of all possible spacetimes of the Universe to the FLRW [37]. The current effort in cosmology is mainly directed towards making a very precise determination of the free parameters of this model [22,38,39]. While the alternative observational approach uses observational data from our past light cone such as apparent luminosities, angular diameters and number count of sources without assuming the cosmological principle to construct the geometry of the Universe [40–42]. The observational approach encounters difficulties due to the absence of the initial data [43]. However, it holds a huge promise that when all the issues are resolved, it will not only provide us with the exact geometry of the Universe, it will also allow us to quantify the homogeneity scale if anything like that exists.

The cosmological fitting approach we describe here is an intermediate approach between these two approaches [44]. It does not assume *a priori* that the FLRW spacetime describes the observable Universe accurately at all times and at all distances, rather it considers it as a fiducial model of the Universe. For example, we assume that the fiducial model is specified by

$$\bar{U} = \{\bar{M}, \bar{g}_{ab}, \bar{u}^a, \bar{\rho}, \bar{N}, \bar{\mu}, \bar{a}_b, \bar{\alpha}_{\parallel}, \bar{\alpha}_{\perp}\}, \quad (1)$$

where  $\bar{M}$  is Riemanian manifold,  $\bar{g}_{ab}$  is the metric,  $\bar{u}^a$  is the four velocity,  $\bar{N}$  is the number count of sources,  $\bar{\mu}$  is the distance-redshift relation (distance modulus),  $\bar{a}_b$  is the intercept of the Hubble diagram,  $\bar{\alpha}_{\parallel}$  and  $\bar{\alpha}_{\perp}$  are the radial and orthogonal components of the Alcock and Paczyński parameters [17]. Then, it takes some hints from the observational approach such that it assumes that there exists a model of the observed Universe that gives a realistic representation of the Universe including all inhomogeneities down to some specified length scale  $|\mathbf{x}_1 - \mathbf{x}_2| > R$

$$U = \{M, g_{ab}, u^a, \rho, N, \mu, a_b, \alpha_{\parallel}, \alpha_{\perp}\}. \quad (2)$$

The task then is to determine a best fit model of the Universe given  $U$ . Just like in the observational approach, the most optimal procedure for obtaining the best fit model is to fit the observed data or observables on the past light cones  $C^-(\bar{p})$  and  $C^-(p)$  of points  $\bar{p}$ ,  $p$  in  $\bar{U}$  and  $U$ , respectively. Since  $\bar{U}$  is homogenous and isotropic, any point is equally likely; for the points in  $U$ , we smooth over angular dependence of any observable,  $X$ , associated with  $U$ , on the past light cone of an observer with four velocity  $u^a$  within a sphere of constant redshift

$$\langle X(z, \hat{\mathbf{n}}) \rangle_{\Omega} = \frac{1}{4\pi} \int d^2\Omega X(z, \hat{\mathbf{n}}) = \int d\hat{\mathbf{n}} X(z, \hat{\mathbf{n}}), \quad (3)$$

where  $\hat{\mathbf{n}}$  is line of sight direction. We assume that the redshift is monotonic for points separated by a distance greater than  $R$ . We compare the monopole of the observable  $X$  obtained by smoothing out anisotropies on the past null cone  $C^-(p)$  to the corresponding prediction by the fiducial model of the same observable. The free parameters of the fiducial model, i.e.,  $\bar{U}$  are then adjusted to obtain the best-fit value to the angular average of the observable in the lumpy universe. In principle, we evaluate the  $\chi^2$  of any observable  $X$ :

$$\chi_X^2 = \sum_i \left[ \frac{\langle X_i \rangle_{\Omega} - \bar{X}(z_i | H_0^X, q_0^X)}{\sigma_i^X} \right]^2, \quad (4)$$

where  $\sigma_i^X$  is the covariance (in a single parameter, it reduces to the variance) and  $H_0$  and  $q_0$  are the Hubble rate and the deceleration parameter, respectively. Then we find the optimum values of  $H_0^X$  and  $q_0^X$  by minimizing the  $\chi_X^2$  with respect to  $H_0^X$  and  $q_0^X$

$$\frac{\partial \chi_X^2}{\partial H_0^X} = 0, \quad \text{and} \quad \frac{\partial \chi_X^2}{\partial q_0^X} = 0. \quad (5)$$

In order to build a complete picture of the best-fit model, the ideal thing we will be to obtain the optimum values of  $H_0$  and  $q_0$  by minimaxing the joint  $\chi^2 = \chi_{\mu}^2 + \chi_{a_b}^2 + \chi_{\alpha_{\parallel}}^2 +$

$\chi_{\alpha_{\perp}}^2 + \dots$  with respect to  $H_0$  and  $q_0$  simultaneously. We do not consider this here because our focus is to identify the source of tension in the inferred Hubble rate. This is best done by independently fitting the late and early Universe observables to their corresponding FLRW space models.

This intermediate approach offers tremendous advantages over the other two approaches, such as the following:

- (i) Clear description of the relevant physics: It makes apparent the geometrical and physical interpretation of the FLRW models we use because it provides a clear link between the highly symmetric fiducial model and more realistic descriptions of the lumpy universe we observe.
- (ii) Delineation of scales: It helps to establish the appropriate scale of validity of the best-fit model of the Universe. That is it helps to address statement that the Universe can be regarded as an almost FLRW universe if averaged out over a specified length scale.
- (iii) Guidance in the presence of tension: It does not only enable one to determine the best-fit FLRW universe model, it allows to predict the presence of tension in the model parameters. For example, under this framework tensions appear in the model parameters when the fiducial model is fit to data from length scales or time in the evolution of the Universe where the background FLRW spacetime is not applicable (i.e., nonlinear scales). We discuss this point in greater detail in the subsequent sections.
- (iv) Wider application: It is possible to use it repeatedly; that is, to consider which of the lumpy universe models  $U$  and another lumpiness model, say  $U'$ , give an even better description of the real Universe than  $U$ , i.e., which one of them describes the inhomogeneities in even more detail.

### A. Inhomogeneous distances in a realistic model of the Universe

We work in the geometric optics limit; i.e., we assume that the wavelength of photon is small compared to the radius of curvature of the Universe. In this limit, null geodesics describes photon propagation and a tangent vector to the null geodesic is given by  $k^a = dx^a/d\lambda$  and it satisfies

$$k_a k^a = 0 \quad \text{and} \quad k^b \nabla_b k^a = 0, \quad (6)$$

where  $\lambda$  is the affine parameter. When initialized at the observer position, it increases monotonically [45].  $\nabla$  is the covariant derivative of the physical spacetime of the Universe. With respect to a set of fundamental comoving observers with the average four velocity  $u^a$ , we can decompose  $k^a$  into parallel and orthogonal components:

$$k^a = (-u_b k^b)(u^a - n^a) = E(u^a - n^a), \quad (7)$$

where  $n^a$  is the line of sight spatial direction vector with a normalization  $n_a n^a = 1$ ,  $E = -u_b k^b$  is the photon energy measured by  $u^a$ .  $n^a$  is orthogonal to  $u^a$ ;  $n_a u^a = 0$ . Note that our choice of  $n^a$  is opposite to the direction of photon propagation.  $k^a$  is pointing along an incoming light ray on the past light cone of the observer. The apparent magnitude of any source,  $m$ , is related to the observed flux density  $F_{d_L}$  measurement at a given luminosity distance  $d_L$  in a given spectral filter according to

$$m = -2.5 \log_{10}[F_{d_L}]. \quad (8)$$

The absolute magnitude,  $M$ , of the same source is defined as the apparent magnitude measured at a distance  $D_F$

$$M = -2.5 \log_{10}[F_{D_F}], \quad (9)$$

where  $F_{D_F}$  is called the reference flux or the zero point of the filter [46–48]. The observed flux density at both distances obey the inverse square law with the luminosity distance,  $d_L$ :  $F_{d_L}/F_{D_F} = [D_F/d_L]^2$ . The distance modulus is defined as the difference between  $m$  and  $M$

$$m - M = -2.5 \log \left[ \frac{F_{d_L}}{F_{D_F}} \right] = 5 \log \left[ \frac{d_L}{D_F} \right] = 5 \log \left[ \frac{d_L}{[\text{pc}]} \right] - 5. \quad (10)$$

In the last equality, we set  $D_F = 10$  pc for historical reasons. In this case, it means that the absolute magnitude is the apparent magnitude if the telescope is placed at a distance of 10 pc. In cosmology however,  $D_F$  is set to  $D_F = 1$  Mpc leading to

$$\mu(z, \hat{\mathbf{n}}) = m(z, \hat{\mathbf{n}}) - M = 5 \log \left[ \frac{d_L}{[\text{Mpc}]} \right] + 25, \quad (11)$$

where  $d_L$  is in the units of Mpc. This implies that, for cosmological purposes, the consistently calibrated cosmic distance ladder would have a reference flux determined at 1 Mpc. The generalized coordinate independent expressions for the area and the luminosity distance at low redshift are (see the Appendix for details of the derivation) [24,49]

$$d_A(z, \hat{\mathbf{n}}) = \frac{z}{[K^c K^d \nabla_c u_d]_o} - \frac{1}{2} \left[ \frac{K^c K^d K^e \nabla_e \nabla_d u_c}{(K^c K^d \nabla_c u_d)^3} \right]_o z^2 + \mathcal{O}(z^3), \quad (12)$$

$$d_L(z, \hat{\mathbf{n}}) = \frac{z}{[K^c K^d \nabla_d u_c]_o} \left\{ 1 + \frac{1}{2} \left[ 4 - \frac{K^c K^d K^e \nabla_e \nabla_d u_c}{(K^c K^d \nabla_c u_d)^2} \right]_o z + \mathcal{O}(z^2) \right\}, \quad (13)$$

where  $K^a$  is a normalized null vector:  $K^a = u^a - n^a$ . The associated null geodesic tangent vector is given by

$k^a = (1+z)K^a$ . In general,  $d_L$  is related to  $d_A$  via distance duality relation:  $d_L = (1+z)^2 d_A$  [50–52]. We neglect the effect of the heliocentric peculiar velocity. Its contribution will not substantially change the determination of the Hubble rate, especially via the local distance ladder [53]. The redshift in Eqs. (12) and (13) corresponds to the cosmological redshifts.

On the FLRW background space, Eqs. (12) and (13) reduce to

$$\bar{d}_A(z) = \frac{z}{H_0} \left[ 1 - \frac{1}{2}(3+q_0)z + \mathcal{O}(z)^2 \right], \quad (14)$$

$$\bar{d}_L(z) = \frac{z}{H_0} \left[ 1 + \frac{1}{2}[1-q_0]z + \mathcal{O}(z)^2 \right]. \quad (15)$$

The magnitude-redshift relation is given by Eq. (11) with the luminosity distance given by Eq. (15). We have truncated the Taylor series expansion at second order in redshift expansion because our focus is on how the cosmic structures impact the measurement of the Hubble rate,  $H_0$  and the deceleration parameters,  $q_0$ . It is certainly debatable whether these series expansions on arbitrary spacetime have much relation with the magnitude-redshift relation in the observable Universe. In particular, is it analytic, especially in the region where shell crossing occurs? These doubts are valid, but this is how we address them:

- (i) Differentiability at  $z = 0$ : We showed in [35] that  $d_A$  expanded up to second order in standard cosmological perturbation theory on an FLRW background spacetime is differentiable at  $z = 0$ . The linearly perturbed FLRW equations can be rewritten in terms of the equations of the exact inhomogeneous Szekeres models [54]. This shows that the generalized inhomogeneous model is also differentiable at  $z = 0$ .
- (ii) Shell crossing singularity: It is likely that, in certain directions, the Taylor series expansion of observables will be multivalued as a light beam passes through collapsing regions, this is a valid concern. We show in Sec. IV A that the collapsing region around the observer can be isolated from the expanding spacetime by setting the smoothing scale at the zero-velocity surface [35]. Similar restriction was deployed recently in an attempt to estimate Eq. (13) from a general relativistic  $N$ -body simulation [55].
- (iii) Convergences of the series expansion: Convergence of series expansion is a problem in general, in our case, it is well known that, for  $z < 0.1$ , Eqs. (14) and (15) converge at second order in redshift expansion. It is likely that, in the presence of structures, a higher-order redshift correction will be needed to achieve convergence at the same redshift. We find some hints of this in [35] but a more detailed study is needed since next to leading order terms were neglected in the analysis. Currently, we are essentially interested in what happens in the limit where

$z \ll 1$  and we have no reason to believe that second-order series expansion in redshift will not be enough to determine the Hubble rate.

### B. Covariant and multipole moment decomposition of observables

We are primarily interested in the multipole moment decomposition of the observable-redshift relations so that the monopole or the all-sky average can be compared to the corresponding expression based on the background FLRW spacetime. To accomplish this, we decompose  $K^a K^b \nabla_a u_b$  and  $K^a K^b K^c \nabla_a \nabla_b u_c$  into irreducible physical quantities that live on the hypersurface orthogonal to  $u^a$  using in  $1 + 3$  covariant decomposition formalism [25,26,51,56–58]. The irreducible decomposition of the spacetime covariant derivative of  $u^a$  for geodesic observers is given by [26,58]

$$\nabla_b u_a = \frac{1}{3} \Theta h_{ab} + \sigma_{ab}, \quad (16)$$

where  $\Theta$  denotes the expansion ( $\Theta > 0$ )/contraction ( $\Theta < 0$ ) of the nearby geodesics associated with  $u^a$ ,  $\sigma_{ab}$  is the shear tensor (it describes the rate of change of the deformation of spacetime in the neighborhood of the observer),  $h_{ab} = g_{ab} + u_a u_b$  is the metric on the hypersurface orthogonal to the timelike  $u^a$  ( $u^a u_a = -1$ ), and  $g_{ab}$  is the physical spacetime metric. The vorticity vanishes for irrotational fluids or geodesic observer. There is a one-to-one mapping between all symmetric trace-free tensors of rank  $\ell$  and the spherical harmonics of order  $\ell$  [27,59–61]. We can see this by decomposing the line of sight direction vector  $n^a$  at the observer position on an orthonormal tetrad basis [60,62]

$$n^a(\theta, \phi) = (0, \sin \theta \sin \phi, \sin \theta \cos \phi, \cos \theta). \quad (17)$$

In the standard spherical harmonics decomposition formalism, any function  $f$  on the sky may be expanded in spherical harmonics,  $Y^{\ell m}(\hat{\mathbf{n}})$  according to

$$\begin{aligned} f(\hat{\mathbf{n}}) &= \sum_{\ell=0}^L \sum_{m=-\ell}^{\ell} F^{\ell m} Y^{\ell m}(\hat{\mathbf{n}}) = \sum_{\ell=0}^{\infty} F_{A_\ell} n^{A_\ell} \\ &= F + F_a n^a + F_{ab} n^a n^b + F_{abc} n^a n^b n^c, \end{aligned} \quad (18)$$

where  $F^{\ell m}$  is the spherical harmonic coefficients.  $A_\ell = a_1 a_2 \dots a_\ell$  is a compound index notation that denotes number of indices,  $F_{A_\ell}$  is the moments: it is symmetric, trace-free, and orthogonal to  $u^a$ ,  $F_{A_\ell} = F_{(A_\ell)}$ ,  $F_{A_\ell ab} h^{ab} = 0$ , and  $F_{A_\ell a} u^a = 0$ , respectively. Here, “ $(\dots)$ ” brackets in the subscript denote the symmetrization overall indices and the angle brackets “ $\langle \dots \rangle$ ” denotes PSTF part. In the second equality, we show an equivalent way of performing the spherical harmonic expansion in projected symmetric trace-free (PSTF) tensors in a  $n^a$  basis [27,59–61]. The PSTF part of any index tensor is given by [27,63–66]

$$\begin{aligned} F_{\langle A_\ell \rangle} &= \sum_{n=0}^{\lfloor \ell/2 \rfloor} \mathcal{B}^{\ell n} h_{(a_1 a_2 \dots a_{2n-1} a_{2n}} F_{a_{2n+1} \dots a_\ell)}, \\ \text{with } \mathcal{B}_{\ell n} &= \frac{(-1)^n \ell! (2\ell - 2n - 1)!!}{(\ell - 2n)! (2\ell - 1)! (2n)!!}. \end{aligned} \quad (19)$$

$\lfloor \ell/2 \rfloor$  means the largest integer part less than or equal to  $\ell/2$ ,  $\ell! = \ell(\ell - 1)(\ell - 2)(\ell - 3) \dots (1)$ , and  $\ell!! = \ell(\ell - 2) \times (\ell - 4)(\ell - 6) \dots (2 \text{ or } 1)$ . The moment and covariant decomposition of  $K^a K^b \nabla_a u_b$  and  $K^a K^b K^c \nabla_a \nabla_b u_c$  within general relativity for dust is given by [8,67,68]

$$K^a K^b \nabla_a u_b = \frac{1}{3} \Theta + \sigma_{ab} n^a n^b, \quad (20)$$

$$K^a K^b K^c \nabla_a \nabla_b u_c = \mathcal{O} + \mathcal{O}_a n^a + \mathcal{O}_{ab} n^a n^b + \mathcal{O}_{abc} n^a n^b n^c, \quad (21)$$

where  $\mathcal{O}$ ,  $\mathcal{O}_a$ ,  $\mathcal{O}_{ab}$ , and  $\mathcal{O}_{abc}$  are the monopole, dipole, quadrupole, and octupole moments of  $K^a K^b K^c \nabla_a \nabla_b u_c$

$$\mathcal{O} = \frac{1}{6} \rho + \frac{1}{3} \Theta^2 - \frac{1}{3} \Lambda + \sigma_{ab} \sigma^{ab}, \quad (22)$$

$$\mathcal{O}_a = \frac{1}{3} \tilde{D}_a \Theta + \frac{2}{5} \tilde{D}_b \sigma_a^b, \quad (23)$$

$$\mathcal{O}_{ab} = E_{ab} + 2\Theta \sigma_{ab} + 3\sigma^c{}_a \sigma_{bc}, \quad (24)$$

$$\mathcal{O}_{abc} = \tilde{D}_a \sigma_{bc}. \quad (25)$$

Here  $\rho$  is the matter density,  $\Lambda$  is the cosmological constant,  $E_{ab}$  is the electric part of the Weyl tensor, and  $\tilde{D}_a$  is the spatial derivative on the hypersurface.  $E_{ab}$  describes how nearby geodesics tear apart from the equation. It is crucial in the discussion that follows. An extension to modified gravity theories and general matter fields should be straightforward.

### III. THE COSMOLOGICAL FITTING PROBLEM

In this section, we consider how surveys that measure the imprints of the BAO in galaxy distribution and the apparent magnitude of the type 1A supernova are compared to a cosmological model through the Alcock-Paczyński parameters, the distance-redshift relation. Our key focus will be to estimate how inhomogeneity affects the determination of the Hubble rate and the deceleration parameter.

#### A. Cosmological fitting problem: Alcock-Paczyński parameters

The BAO scale constitutes an important link between the physics, before and around the drag and present epoch. Similar to the cosmic microwave background radiation (CMB), the plasma physics of acoustic density waves before decoupling imprints a characteristic scale in the

matter distribution. The characteristic scale, i.e., BAO scale, appears as an excess in the probability of finding galaxies separated by some distance in the distribution of sources seen today on the sky. Since a fiducial model for the separation is required for calculating the separation between galaxies, Alcock and Paczyński [17] introduced a clever way to recover the true separation. For a spherical symmetric distribution of sources, the two-point correlation function,  $\xi_g$ , is given by [69]

$$\xi_g(r_{12\parallel}, r_{12\perp}) = \frac{1}{\alpha_{\parallel}\alpha_{\perp}^2} \xi_g(\alpha_{\parallel}r_{12\parallel}^{\text{fid}}, \alpha_{\perp}r_{12\perp}^{\text{fid}}), \quad (26)$$

where  $r_{12}$  and  $r_{12}^{\text{fid}}$  are the true and fiducial separation between two galaxies, respectively. Within the cosmological standard model treatment, the difference between the fiducial model and true model are parametrized by

$$\bar{\alpha}_{\parallel} = \frac{\bar{H}^{\text{fid}}}{\bar{H}}, \quad \bar{\alpha}_{\perp} = \frac{\bar{d}_A}{\bar{d}_A^{\text{fid}}}. \quad (27)$$

Here  $\bar{H}^{\text{fid}}$  and  $\bar{d}_A^{\text{fid}}$  are the fiducial Hubble rate and area distance, respectively.  $\bar{H}$  and  $\bar{d}_A$  are then adjusted to obtain the best-fit to the observed data. BAO is sensitive to the Hubble rate through the distortions ( $\alpha_{\parallel}$  and  $\alpha_{\perp}$ ) at the survey mean redshift  $z$ . The determination of the value of the Hubble rate today is made assuming a model. The measurement of the monopole of Eq. (26) constrains  $\alpha = \alpha_{\perp}^{2/3}\alpha_{\parallel}^{1/3}$  [18,70], while the quadrupole moment is most sensitive to the Alcock-Paczyński ratio  $\epsilon = \alpha_{\perp}/\alpha_{\parallel}$  [69]. Using the void-galaxy cross-correlation from the BOSS survey at the mean redshift of  $z = 0.57$ , [69] finds a strong constraint on  $\alpha_{\perp}/\alpha_{\parallel} = 1.016 \pm 0.011$  using the CMASS galaxy sample of the BOSS DR12 data release. This constraint when interpreted within the  $\Lambda$ CDM model [i.e., Eq. (27) with the sound horizon,  $r_s$ , set to the Planck value] is consistent with the Planck collaboration's determination of  $H_0$  from the analysis of the anisotropies in the CMB [22]:

$$H_0 = 67.4 \pm 0.5 \text{ km/sec/Mpc}. \quad (28)$$

In a lumpy universe, the structure of Eq. (26) will change slightly, however, it holds for a spherical symmetric distribution of sources. We will discuss modifications away from this limit elsewhere. For an almost FLRW spacetime for which we are interested here, Eq. (27) generalizes as follows:

$$\alpha_{\parallel} = \frac{\partial r_{\parallel}}{\partial r_{\parallel}^{\text{fid}}} = \frac{\partial r_{\parallel}}{\partial z} \frac{\partial z}{\partial r_{\parallel}^{\text{fid}}} \simeq \frac{d\lambda}{dz} \frac{dz}{d\lambda^{\text{fid}}}, \quad (29)$$

$$= \frac{\bar{H}^{\text{fid}}}{\bar{H}} \left[ 1 + \frac{\sigma_{ab}}{\bar{H}} n^a n^b \right]^{-1}, \quad (30)$$

$$= \frac{\bar{H}^{\text{fid}}}{\bar{H}} \left[ 1 - \frac{\sigma_{ab}}{\bar{H}} n^a n^b + \frac{\sigma_{ab}\sigma_{cd}}{\bar{H}\bar{H}} n^a n^b n^c n^d + \mathcal{O}(\sigma^4) \right], \quad (31)$$

where  $H = \Theta/3$  in the last equality. This is the Hubble rate associated with the expansion of the nearby congruence in a lumpy universe. Moreover, we assumed that the real Universe is almost statistically homogeneous and isotropic, i.e.,  $\sigma_{ab}n^a n^b/H \ll 1$ . To move from the first line of Eq. (29) to the second, we made use of the propagation equation for the redshift [71]

$$\frac{dz}{d\lambda} = -(1+z)^2 [H + \sigma_{ab}n^a n^b], \quad (32)$$

$$\frac{dz}{d\lambda^{\text{fid}}} = -(1+z)^2 \bar{H}^{\text{fid}}. \quad (33)$$

Note that on the fiducial FLRW spacetime, the shear vanishes  $\sigma_{ab} = 0$ . At low redshift, the generalized counterpart to  $\bar{\alpha}_{\perp}$  involves replacing the background area distance with Eq. (12).

To obtain the best-fit model from the radial component of the separation in the limit  $z \rightarrow 0$ , we compare  $\bar{\alpha}_{\parallel}$  to the all-sky average of  $\alpha_{\parallel}$

$$\bar{\alpha}_{\parallel} = \langle \alpha_{\parallel} \rangle_{\Omega} = \frac{\bar{H}^{\text{fid}}}{\bar{H}} \left[ 1 + \left\langle \frac{\sigma_{ab}\sigma_{cd}}{\bar{H}\bar{H}} n^a n^b n^c n^d \right\rangle_{\Omega} + \mathcal{O}(\sigma^4) \right], \quad (34)$$

$$= \frac{\bar{H}^{\text{fid}}}{\bar{H}} \left[ 1 + \frac{2}{15} \frac{\sigma_{ab}\sigma^{ab}}{\bar{H}^2} + \mathcal{O}(\sigma^4) \right]. \quad (35)$$

To perform the all-sky average we decompose  $\sigma_{(ab}\sigma_{cd)}$  into an irreducible unit and then extract the monopole using

$$\begin{aligned} n^a n^b n^c n^d \sigma_{(ab}\sigma_{cd)} &= n^a n^b n^c n^d \langle \sigma_{(ab}\sigma_{cd)} \rangle \\ &+ \frac{4}{7} n^a n^b \sigma_{(a}^c \sigma_{b)c} + \frac{2}{15} \sigma_{ab}\sigma^{ab}. \end{aligned} \quad (36)$$

This can also be done by performing the angular integration in Eq. (34) right away [28]. Comparing Eq. (27) to Eq. (35), we obtain the effective Hubble rate

$$H^{\alpha_{\parallel}} = \bar{H} \left[ 1 - \frac{2}{15} \frac{\sigma_{ab}\sigma^{ab}}{\bar{H}^2} + \mathcal{O}(\sigma^4) \right]. \quad (37)$$

The Hubble rate inferred from the constraint on  $\alpha_{\parallel}$  is biased by  $-2\sigma_{ab}\sigma^{ab}/15\bar{H}^2$ . For the orthogonal component,  $\alpha_{\perp}$ , we focus on  $d_A$ , since the fiducial model is the same, it is reduced to comparing Eq. (14) to the all-sky average of Eq. (12) at a fixed redshift. At the leading order in redshift, the effective Hubble rate from fitting the monopole of area distance in a lumpy universe to the FLRW spacetime is given by

$$\begin{aligned} \frac{1}{H_0^{d_A}} &= \left\langle \frac{1}{H_0} \left( 1 + \frac{\sigma_{ab}}{H_0} n^a n^b \right)^{-1} \Big|_{z=z_o} \right\rangle_{\Omega} \\ &= \frac{1}{H_0} \left[ 1 - \frac{\sigma_{(ab)}}{H_0} n^a n^b + \frac{\sigma_{(ab}\sigma_{cd)}}{H_0 H_0} n^a n^b n^c n^d + \mathcal{O}(\sigma^4) \right], \end{aligned} \quad (38)$$

where  $\Theta_o = 3H_0$  is the monopole component of  $K^a K^b \nabla_a u_b$ . Again, we expanded  $(K^a K^b \nabla_a u_b)^{-1}$  up to second order in  $\sigma_{ab} n^a n^b / H_0 \ll 1$ . Using Eq. (36) again and noting that  $\sigma^a_a = 0$ , we find

$$\frac{1}{H_0^{d_A}} \equiv \frac{1}{H_0} \left[ 1 + \frac{2}{15} \frac{\sigma_{ab}\sigma^{ab}}{H^2} \Big|_{z_o} + \mathcal{O}(\sigma^4) \right]. \quad (39)$$

The Hubble rate inferred from the area distance by fitting the area distance information from the lumpy universe to an FLRW background spacetime is given by

$$H_0^{d_A} = H_0 \left[ 1 - \frac{2}{15} \frac{\sigma_{ab}\sigma^{ab}}{H^2} \Big|_{z_o} + \mathcal{O}(\sigma^4) \right]. \quad (40)$$

Furthermore, the evolution of  $\sigma_{ab}$  is sourced by the electric part of the Weyl tensor,  $E_{ab}$  [26,58]

$$\frac{D\sigma_{ab}}{D\tau} = -\frac{2}{3}\Theta\sigma_{ab} - \sigma^c_{\langle a}\sigma_{b\rangle c} - E_{ab}. \quad (41)$$

Again,  $E_{ab}$  contains information about the tidal forces due to gravity, it represents how nearby geodesics tear apart from each other [58]. In an almost FLRW spacetime (i.e., small perturbation on top of an FLRW spacetime),  $\sigma_{ij}$  is related to  $E_{ij}$  in comoving spacetime

$$\sigma_{ij}(\eta, \mathbf{x}) \sim - \int_{\eta_{\text{ini}}}^{\eta} d\eta' E_{ij}(\eta', \mathbf{x}'). \quad (42)$$

In this form, it is straightforward to see that  $\sigma_{ij}$  describes the cumulative effect of the local geometry deformation from the initial seed time to the time of observation. It also helps to understand why  $\sigma_{ij}$  characterizes the cosmic web more transparently than  $E_{ij}$  [72,73].

For the deceleration parameter today, we compare Eq. (14) to the monopole of Eq. (12) at the second order in redshift

$$\frac{(3 + q_0^{d_A})}{H_0^{d_A}} = \left\langle \frac{K^a K^b K^c \nabla_a \nabla_b u_c}{(K^a K^b \nabla_a u_b)^3} \right\rangle_{\Omega}. \quad (43)$$

Decomposing the denominator in terms of the expansion and shear tensor and expressing the result into irreducible unit, we found

$$\begin{aligned} (K^a K^b \nabla_a u_b|_0)^3 &= \frac{1}{27}\Theta^3 + \frac{1}{3}\Theta^2\sigma_{ab} + \sigma_{ab}\sigma_{cd}\Theta n^a n^b n^c n^d \\ &\quad + \mathcal{O}(\sigma^3), \end{aligned} \quad (44)$$

$$\begin{aligned} &= \mathcal{H}^{(3)} + \mathcal{H}^{(3)}_{ab} n^a n^b + \mathcal{H}^{(3)}_{abcd} n^a n^b n^c n^d \\ &\quad + \mathcal{O}(\sigma^3). \end{aligned} \quad (45)$$

In the second equality, we have introduced the first few multipole moments as

$$\mathcal{H}^{(3)} = H^3 \left( 1 + \frac{6}{15} \frac{\sigma_{ab}\sigma^{ab}}{H^2} \right), \quad (46)$$

$$\mathcal{H}^{(3)}_{ab} = \frac{1}{3}\Theta^2\sigma_{ab} + \frac{4}{7}\sigma^c_{\langle a}\sigma_{b\rangle c}\Theta, \quad (47)$$

$$\mathcal{H}^{(3)}_{abcd} = \sigma_{\langle ab}\sigma_{cd\rangle}\Theta. \quad (48)$$

Here  $\mathcal{H}^{(3)}$  is the monopole and  $\mathcal{H}^{(3)}_{ab}$  and  $\mathcal{H}^{(3)}_{abcd}$  are the quadrupole and the hexadecapole moments of  $(K^a K^b \nabla_a u_b|_0)^3$ , respectively. Using Eqs. (21) and (45) we find that the best-fit deceleration parameter is given by

$$\begin{aligned} q_0^{d_A} &= -3 + \frac{H_0^{d_A}}{\mathcal{H}^{(3)}} \left[ \mathcal{O} \left( 1 + \frac{2}{15} \frac{\mathcal{H}^{(3)}_{ab}\mathcal{H}^{(3)ab}}{\mathcal{H}^{(3)2}} \right) \right. \\ &\quad \left. - \frac{2}{15} \frac{\mathcal{H}^{(3)}_{ab}}{\mathcal{H}^{(3)}} \mathcal{O}^{ab} \right] \Big|_{z=z_o}, \end{aligned} \quad (49)$$

$$\begin{aligned} &\approx \frac{1}{H^2} \left\{ \frac{1}{6}\rho - \frac{1}{3}\Lambda + \frac{3}{5}\sigma_{ab}\sigma^{ab} \right. \\ &\quad \left. + \frac{2}{3} \left( \frac{1}{6}\rho - \frac{1}{3}\Lambda \right) \frac{\sigma^{ab}\sigma_{ab}}{H^2} - \frac{2\sigma^{ab}E_{ab}}{5H} \right\} \Big|_{z=z_o}. \end{aligned} \quad (50)$$

Given that the distance duality relation or Etherington reciprocity theorem holds, the Hubble and deceleration parameters obtained from the monopole of luminosity distance must correspond to the Hubble rate given in Eqs. (40) and (50), respectively [74]. We checked and find that this holds, thus for the Hubble rate  $H_0^{d_L} = H_0^{d_A}$  and the deceleration parameter  $q_0^{d_L} = q_0^{d_A}$ .

## B. Cosmological fitting problem: Distance modulus

The CCHP uses the distance modulus with the luminosity distance given by the flat FLRW spacetime (15) to estimate  $H_0$  and  $q_0$  [15].

$$\mu(z, H_0, q_0) = m - M, \quad (51)$$

$$\begin{aligned} &= 5\log_{10} d_L + 25 \\ &= 5\log_{10} \left[ \frac{z}{H_0} \left( 1 + \frac{1}{2}(1 - q_0)z + \mathcal{O}(z^2) \right) \right] \\ &\quad + 25. \end{aligned} \quad (52)$$

One unique feature of the CCHP approach is that it uses the TRGB to calibrate the SNIa samples. According to [75], the best-fit  $H_0$  depends crucially on the accuracy with which the absolute magnitude of the SNIa is calibrated

$$M = m - \mu_0^{\text{TRGB}}, \quad (53)$$

where  $m$  is the apparent magnitude of the peak of the SNIa light curve for a given subsample of SNIa colocated with the TRGB,  $\mu_0^{\text{TRGB}}$  is the true calibrator distance modulus. After calibrating  $M$  [15,76], Eq. (51) is used for the SNIa sample in the Hubble flow [i.e., within the redshift range ( $0.03 \leq z \leq 0.4$ )]. CCHP usually put uninformative prior (the value of  $q_0$  does not vary in the model estimates of distance to each of the SNIa in the sample) on  $q_0 = -0.53$  to determine the Hubble rate to be [15]

$$H_0 = 69.6 \pm 1.9 \text{ km/sec/Mpc}. \quad (54)$$

The generalized form of the distance modulus is obtained by replacing  $d_L$  given in (15) with the generalized form given Eq. (13). We then compare the all-sky average to Eq. (51)

$$\langle \mu \rangle_\Omega = \langle m \rangle_\Omega - \langle M \rangle_\Omega = 5 \langle \log_{10}[d_L(z, \hat{\mathbf{n}})] \rangle_\Omega + 25. \quad (55)$$

Comparing Eqs. (55) and (51) requires that we perform the angular integration over logarithm of  $d_L$

$$\langle \log_{10} d_L(z, \hat{\mathbf{n}}) \rangle_\Omega = -\langle \log_{10}[K^c K^d \nabla_d u_c] \rangle_\Omega + \langle \log_{10}[\hat{d}_L(z, \hat{\mathbf{n}})] \rangle_\Omega, \quad (56)$$

where we have used the quotient rule for logarithm to rewrite Eq. (13). We have also introduced the generalized form of the normalized luminosity distance

$$\hat{d}_L(z, \hat{\mathbf{n}}) = z \left\{ 1 + \frac{1}{2} \left[ 4 - \frac{K^c K^b K^a \nabla_a \nabla_b u_c}{(K^c K^b \nabla_c u_b)^2} \right]_0 z + \mathcal{O}(z^2) \right\}. \quad (57)$$

In order to simplify  $\langle \log_{10}[K^c K^d \nabla_d u_c] \rangle_\Omega$  further, we use the irreducible decomposition of  $K^a K^b \nabla_a u_b$

$$\begin{aligned} \log_{10}[K^a K^b \nabla_a u_b|_0] &= \log_{10} \left[ H_0 \left( 1 + \frac{\sigma_{ab}}{H_0} n^a n^b \right) \right] \\ &= \log_{10} H_0 + \log_{10} \left( 1 + \frac{\sigma_{ab}}{H_0} n^a n^b \right). \end{aligned} \quad (58)$$

For  $\sigma_{ab} n^a n^b / H_0 \ll 1$ , we can expand the second term in Taylor series and use Eq. (36) to obtain the PSTF part

$$\log_{10} \left( 1 + \frac{\sigma_{ab}}{H_0} n^a n^b \right) = \frac{1}{\log 10} \left[ \frac{\sigma_{ab}}{H_0} n^a n^b - \frac{1}{2} \frac{\sigma_{ab} \sigma_{cd}}{H_0^2} n^a n^b n^c n^d + \mathcal{O}(\sigma^3) \right], \quad (59)$$

$$= \frac{1}{\log 10} \left[ -\frac{1}{15} \frac{\sigma_{ab} \sigma^{ab}}{H_0^2} + \left( \frac{\sigma_{ab}}{H_0} - \frac{2\sigma_{(a}^c \sigma_{b)c}}{H_0^2} \right) n^{(a} n^{b)} - \frac{1}{2} \frac{\sigma_{(ab} \sigma_{cd)}}{H_0^2} n^{(a} n^b n^c n^{d)} + \mathcal{O}(\sigma^3) \right]. \quad (60)$$

Now it straightforward to perform the all-sky average to obtain the monopole

$$\langle \log_{10}[K^a K^b \nabla_a u_b|_0] \rangle_\Omega = \log_{10} H_0 - \log_{10} \left[ 1 + \frac{1}{15} \frac{\sigma_{ab} \sigma^{ab}}{H_0^2} \right]. \quad (61)$$

Extracting the monopole of  $\langle \log_{10}[\hat{d}_L(z, \hat{\mathbf{n}})] \rangle_\Omega$  is a little more algebraically more involved. We go through it step by step. First, we decompose  $\hat{d}_L(z, \hat{\mathbf{n}})$  in multipole moments

$$\hat{d}_L(z, \hat{\mathbf{n}}) = \sum_{\ell=0}^{\infty} \hat{d}_{A_\ell}(z) n^{(A_\ell)} = \hat{d}_0^L + \hat{d}_a^L n^a + \hat{d}_{ab}^L n^a n^b + \hat{d}_{abc}^L n^a n^b n^c + \mathcal{O}(\hat{d}_{A_{\ell>3}}^L), \quad (62)$$

where  $\hat{d}_0^L$ ,  $\hat{d}_a^L$ , and  $\hat{d}_{ab}^L$  are the monopole, dipole, and quadrupole moments of the Hubble rate-normalized luminosity distance, respectively. Then by factoring out the monopole of  $\hat{d}_L$  and requiring that  $\hat{d}_{A_{\ell>1}}^L / \hat{d}_0^L \ll 1$  allows us to expand the anisotropic part on the background of its monopole moment

$$\log_{10}(\hat{d}_L(z, \hat{\mathbf{n}})) = \log_{10} \hat{d}_0^L + \frac{1}{\log 10} \left[ \frac{\hat{d}_a^L}{\hat{d}_0^L} n^a + \frac{\hat{d}_{ab}^L}{\hat{d}_0^L} n^a n^b - \frac{1}{2} \left( \frac{\hat{d}_a^L \hat{d}_b^L}{\hat{d}_0^L \hat{d}_0^L} n^a n^b + \frac{\hat{d}_{ab}^L \hat{d}_{cd}^L}{\hat{d}_0^L \hat{d}_0^L} n^a n^b n^c n^d \right) + \mathcal{O} \left( \frac{\hat{d}_{A_\ell}^L}{\hat{d}_0^L} \right)^3 \right]. \quad (63)$$

Then taking the all-sky average leads to

$$\langle \log_{10}(\hat{d}_L(z, \hat{\mathbf{n}})) \rangle_{\Omega} = \log_{10} \hat{d}_0^L - \frac{1}{2} \frac{1}{\log 10} \left( \frac{2}{15} \frac{\hat{d}_{ab}^L \hat{d}_L^{ab}}{\hat{d}_0^L \hat{d}_0^L} + \frac{1}{3} \frac{\hat{d}_a^L \hat{d}_L^a}{\hat{d}_0^L \hat{d}_0^L} \right) + \mathcal{O} \left( \frac{\hat{d}_{A_L}^L}{\hat{d}_0^L} \right)^3. \quad (64)$$

We neglect the contribution of the second term since their contribution is second order in redshift  $\mathcal{O}(z^2)$

$$\frac{\hat{d}_{ab}^L \hat{d}_L^{ab}}{\hat{d}_0^L \hat{d}_0^L} = \frac{\hat{d}_a^L \hat{d}_L^a}{\hat{d}_0^L \hat{d}_0^L} \approx 0. \quad (65)$$

We can now make use of the product rule for logarithms to rewrite  $\langle \log_{10} \hat{d}_L(z, \hat{\mathbf{n}}) \rangle_{\Omega}$  as

$$\langle \log_{10} \hat{d}_L(z, \hat{\mathbf{n}}) \rangle_{\Omega} = \log_{10} cz + \log_{10} \left\{ 1 + \frac{1}{2} \left[ 4 - \left\langle \frac{K^c K^b K^a \nabla_a \nabla_b u_c}{(K^c K^b \nabla_c u_b)^2} \right\rangle_{\Omega} z \right] + \mathcal{O}(z^2) \right\}. \quad (66)$$

We simplify this further by first decomposing the denominator into irreducible parts

$$(K^a K^b \nabla_a u_b|_0)^2 = \frac{1}{9} \Theta^2 + \frac{2}{3} n^a n^b \sigma_{ab} \Theta + n^a n^b n^c n^d \sigma_{ab} \sigma_{cd}, \quad (67)$$

$$= \mathcal{H}^{(2)} + n^{(a} n^{b)} \mathcal{H}^{(2)}{}_{(ab)} + n^{(a} n^b n^c n^{d)} \mathcal{H}^{(2)}{}_{(abcd)}, \quad (68)$$

where  $\mathcal{H}^{(2)}$  is the monopole,  $\mathcal{H}^{(2)}{}_{(ab)}$  is the normalized quadrupole and  $\mathcal{H}^{(2)}{}_{(abcd)}$  is the hexadecapole

$$\mathcal{H}^{(2)} = \frac{1}{9} \Theta^2 + \frac{2}{15} \sigma_{ab} \sigma^{ab} = H^2 \left( 1 + \frac{2}{15} \frac{\sigma_{ab} \sigma^{ab}}{H^2} \right), \quad (69)$$

$$\mathcal{H}^{(2)}{}_{(ab)} = \frac{4}{7} \sigma_{(a}^c \sigma_{b)c} + \frac{2}{3} \Theta \sigma_{(ab)}, \quad (70)$$

$$\mathcal{H}^{(2)}{}_{(abcd)} = \sigma_{(ab} \sigma_{cd)}. \quad (71)$$

Therefore, the monopole of the argument of the second term in Eq. (66) becomes

$$\left\langle \frac{K^c K^b K^a \nabla_a \nabla_b u_c}{(K^c K^b \nabla_c u_b)^2} \right\rangle_{\Omega} = \frac{1}{\mathcal{H}^{(2)}} \left[ \mathcal{O} \left( 1 + \frac{2}{15} \frac{\mathcal{H}^{(2)}{}_{ab} \mathcal{H}^{(2)ab}}{\mathcal{H}^{(2)2}} \right) - \frac{2}{15} \frac{\mathcal{H}^{(2)}{}_{ab}}{\mathcal{H}^{(2)}} \mathcal{O}^{ab} \right], \quad (72)$$

$$= 3 + \frac{1}{H^2} \left\{ \frac{1}{6} \rho - \frac{1}{3} \Lambda + \frac{3}{5} \sigma_{ab} \sigma^{ab} + \frac{6}{15} \left[ \frac{1}{6} \rho - \frac{1}{3} \Lambda \right] \left[ \frac{\sigma_{(ab)} \sigma^{(ab)}}{H^2} \right] - \frac{4}{15} \frac{\sigma^{(ab)} E_{(ab)}}{H} \right\}. \quad (73)$$

Finally, we find that the monopole of the logarithm of the Hubble rate normalized luminosity distance is given by

$$\langle \log_{10} \hat{d}_L(z, \hat{\mathbf{n}}) \rangle_{\Omega} = \log_{10} \left\{ z \left[ 1 + \frac{1}{2} \left[ 1 - \frac{1}{H^2} \left( \frac{1}{6} \rho - \frac{1}{3} \Lambda + \frac{3}{5} \sigma_{ab} \sigma^{ab} + \frac{6}{15} \left[ \frac{1}{6} \rho - \frac{1}{3} \Lambda \right] \frac{\sigma_{(ab)} \sigma^{(ab)}}{H^2} - \frac{4}{15} \frac{\sigma^{(ab)} E_{(ab)}}{H} \right) \right] z + \mathcal{O}(z^2) \right] \right\}. \quad (74)$$

Putting everything back to Eq. (55), we find that the monopole of the distance modulus is given by

$$\langle \mu \rangle_{\Omega} = \langle m \rangle_{\Omega} - \langle M \rangle_{\Omega}^R = 25 + 5 \log_{10} \left\{ \frac{1}{H_0^{\mu}} \left[ z \left( 1 + \frac{1}{2} (1 - q^{\mu}) z + \mathcal{O}(z^2) \right) \right] \right\}, \quad (75)$$

where the following terms were defined by comparing to the equivalent FLRW expression given in Eqs. (51) and (52)

$$\langle M \rangle_{\Omega}^R = \langle M \rangle_{\Omega} + 5 \log_{10} \left[ 1 + \frac{1}{15} \frac{\sigma_{ab} \sigma^{ab}}{H^2} \Big|_{z=0} \right], \quad (76)$$

$$H_0^\mu = H_0, \quad (77)$$

$$q^\mu = \frac{1}{H^2} \left( \frac{1}{6}\rho - \frac{1}{3}\Lambda + \frac{3}{5}\sigma_{ab}\sigma^{ab} + \frac{2}{3} \left[ \frac{1}{6}\rho - \frac{1}{3}\Lambda \right] \frac{\sigma_{(ab)}\sigma^{(ab)}}{H^2} - \frac{4}{15} \frac{\sigma^{(ab)}E_{(ab)}}{H} \right) \Big|_{z=0}. \quad (78)$$

This indicates that the best-fit absolute magnitude  $\langle M \rangle_\Omega^R$  of the SNIa includes the effect of tidal deformation of the local geometry. Stated differently, the measurement of the Hubble rate via the local distance ladder accounts for the impact of tidal deformation on the luminosity distance. The Hubble rate determined using the local distance ladder with a properly calibrated absolute magnitude corresponds to the global volume expansion.

### C. Cosmological fitting problem: Intercept of the Hubble diagram

On the other hand, the SHOES collaboration uses the Cepheid variable stars to calibrate the absolute magnitude of the SNIa. The estimate of the Hubble rate is obtained from the constraint on the intercept of the magnitude-redshift relation with the luminosity distance given by the flat FLRW spacetime. Starting from Eq. (11), they rewrite the distance modulus as follows [12]:

$$m = M + 25 + 5 \log_{10} \bar{d}_L = -5a_b + 5 \log_{10} \hat{d}_L(z), \quad (79)$$

where  $a_b$  is the intercept of the of the Hubble diagram and  $\hat{d}_L$  is the Hubble parameter normalized luminosity distance:

$$5a_b = -(M_b + 25 - 5 \log_{10} H_0), \quad (80)$$

$$\hat{d}_L(z) = z \left[ 1 + \frac{1}{2}(1 - q_0)z + \mathcal{O}(z^2) \right]. \quad (81)$$

The Hubble rate is then determined from Eq. (80)

$$\log_{10} H_0 = \frac{M_b + 25 + 5a_b}{5}, \quad (82)$$

where  $M_b$  is called standardizable absolute luminosity in [12], but it does the same job as Eq. (53) in CCHP

$$M_b = m_{b,\text{SNIa}} - \mu_{0,\text{ceph}}, \quad (83)$$

where  $\mu_{0,\text{ceph}}$  is an independent distance modulus to Cepheids and  $m_{b,\text{SNIa}}$  is the apparent magnitude of a subsample of nearby SNIa that live in the same host as the Cepheids. The SHOES collaboration has since made use of different geometrical distance estimates such as the NGC 4258 obtained by modeling the water masers in the nucleus of the galaxy orbit about its supermassive black hole [14], the large magellanic cloud using eclipsing binary systems composed of late-type stars [13], and Milky Way Cepheids

using parallax methods [77,78] to calibrate  $M_b$ . Even though the SHOES collaboration limits the type Ia supernova sample to  $z = 0.023$  due to systematics associated with disentangling the peculiar velocities of the sources from the coherent Hubble flow, they have accurate information on the intercept

$$a_b = \log_{10} \left\{ cz \left[ 1 + \frac{1}{2}(1 - q_0)z + \mathcal{O}(z^3) \right] \right\} - 0.2M_b, \quad (84)$$

$$\approx \log_{10} cz - 0.2M_b. \quad (85)$$

Similarly, the SHOES collaboration puts uninformative prior on  $\bar{q}_0 = -0.55$  [79] to determine  $a_b = 0.71273 \pm 0.00176$ . With the constraint on  $M_b$ , they found that the Hubble rate is given by [80,81]

$$H_0 = 73.1 \pm 1.4 \text{ kms}^{-1} \text{ Mpc}^{-1}. \quad (86)$$

Note that the quoted error here are the error associated with the determination of  $a_b$  and  $M_b$  added in quadrature [12].

We will now show how the approach taken by the SHOES collaboration may be generalized to apply to arbitrary inhomogeneous models. The key ingredient in the generalized expression is the luminosity distance given in Eq. (13). Starting from Eq. (11) and following similar steps that starts from Eq. (79) in the FLRW limit

$$\langle m \rangle_\Omega = \langle M \rangle_\Omega - 5 \langle \log_{10} [K^c K^d \nabla_{d u_c}] \rangle_\Omega + 5 \langle \log_{10} [\hat{d}_L(z, \hat{\mathbf{n}})] \rangle_\Omega + 25, \quad (87)$$

$$= -5 \langle a_b \rangle_\Omega + 5 \langle \log_{10} \hat{d}_L(z, \hat{\mathbf{n}}) \rangle_\Omega, \quad (88)$$

where  $\hat{d}_L(z, \hat{\mathbf{n}})$  is given in Eq. (57) and the generalized intercept is given by

$$\langle a_b(\hat{\mathbf{n}}) \rangle_\Omega = -\frac{1}{5} (\langle M \rangle_\Omega + 25 - 5 \langle \log_{10} [K^a K^b \nabla_a u_b] \rangle_\Omega). \quad (89)$$

Recall that the decomposition of  $\langle K^a K^b \nabla_a u_b \rangle_\Omega$  is discussed between Eqs. (58)–(61). Putting this back into Eq. (89) gives

$$\langle a_b(\hat{\mathbf{n}}) \rangle_\Omega = -\frac{1}{5} (\langle M \rangle_\Omega^R + 25 - 5 \log_{10} H_0), \quad (90)$$

where we have introduced a renormalized absolute magnitude defined in Eq. (76). Similarly, the Hubble rate depends

on the monopole of the intercept and renormalized absolute luminosity according to

$$\log_{10} H_0 = \frac{\langle M \rangle_{\Omega}^R + 25 + 5\langle a_b \rangle_{\Omega}}{5}. \quad (91)$$

$\langle a_b \rangle_{\Omega}$  is obtained independently by fitting to the intercept of the distance modulus of the SNIa peak magnitudes. The intercept of the distance modulus constrains  $\langle M \rangle_{\Omega}^R + 5\langle a_b \rangle_{\Omega}$ , from where we find

$$\langle a_b(\hat{\mathbf{n}}) \rangle_{\Omega} = \langle \log_{10} \hat{d}_L(z, \hat{\mathbf{n}}) \rangle_{\Omega} - 0.2\langle M \rangle_{\Omega}^R, \quad (92)$$

$$\approx \log_{10} \left\{ cz \left[ 1 + \frac{1}{2} \left[ 4 - \left\langle \frac{K^c K^b K^a \nabla_a \nabla_b u_c}{(K^c K^b \nabla_c u_b)^2} \right\rangle_{\Omega} \right] \right] z + \mathcal{O}(z^2) \right\} - 0.2\langle M \rangle_{\Omega}^R, \quad (93)$$

$$= \log_{10} \left\{ cz \left[ 1 + \frac{1}{2} \left[ 1 - \frac{1}{H^2} \left( \frac{1}{6}\rho - \frac{1}{3}\Lambda + \frac{3}{5}\sigma_{ab}\sigma^{ab} + \frac{6}{15} \left[ \frac{1}{6}\rho - \frac{1}{3}\Lambda \right] \frac{\sigma_{(ab)}\sigma^{(ab)}}{H^2} - \frac{4}{15} \frac{\sigma^{(ab)}E_{(ab)}}{H} \right) \right] \right] z + \mathcal{O}(z^2) \right\} - 0.2\langle M \rangle_{\Omega}^R, \quad (94)$$

$$\approx \log_{10} cz - 0.2\langle M \rangle_{\Omega}^R. \quad (95)$$

where we made use of Eq. (66) in the second equality; in the third equality, we used Eq. (74) and the very low redshift approximation is enough [12].

Finally, we remark that the Hubble rate and the deceleration parameter obtained from fitting to the monopole of the Alcock-Paczyński parameters for the BAO signal in the two-point correlation function agree:

$$H_0^{d_L} = H_0^{d_A} = H_0^{\alpha_{||}}, \quad (96)$$

$$q_0^{d_L} = q_0^{d_A}. \quad (97)$$

But they differ from the local cosmic distance ladder measurement determination

$$H_0^{\mu_l} = H_0^{\mu}, \quad (98)$$

$$q_0^{\mu_l} = q_0^{\mu}. \quad (99)$$

The Hubble rate from the local cosmic distance measurement corresponds to volume expansion without any contamination due to the tidal deformation of the local spacetime geometry. The Hubble rate and the deceleration parameter determined from the local cosmic ladder and Alcock-Paczyński parameters of the BAO signal differ according to

$$H_0^{d_A} - H_0^{\mu} \approx -\frac{2}{15} \frac{\sigma_{ab}\sigma^{ab}}{H} \Big|_{z=0} + \mathcal{O}(\sigma^3), \quad (100)$$

$$q_0^{d_A} - q_0^{\mu} \approx -\frac{2}{15} \frac{\sigma^{(ab)}E_{(ab)}}{H^2} \Big|_{z=0} + \mathcal{O}(\sigma^3). \quad (101)$$

It is possible to calibrate the SNIa using the BAO distance information (proper distance traveled by the acoustic waves from the initial time to the last scattering surface) instead of the nearby distance anchors [82]. This approach usually involves the use of a model that does not include the tidal fields we discussed here in the calibration process [83], thus, we can associate the absolute magnitude of the SNIa determined through this process to  $\langle M \rangle_{\Omega}$ . On the other hand, the local cosmic distance ladder approach does not assume any model for distance (apart from the parallax formula for distance, flux inverse square law, period-luminosity relation for Cepheids) during the calibration process, hence, we can associate the absolute magnitude it determines to  $\langle M \rangle_{\Omega}^R$ . The difference is given by

$$\langle M \rangle_{\Omega}^R - \langle M \rangle_{\Omega} \approx \frac{1}{3 \log 10} \frac{\sigma_{ab}\sigma^{ab}}{H^2} \Big|_{z=0} + \mathcal{O}(\sigma^3). \quad (102)$$

#### IV. THE PERTURBED FLRW SPACETIME

The results we have derived so far by fitting the FLRW model to an inhomogeneous model is general, they apply to any inhomogeneous cosmological model provided that anisotropies are small when compared to the monopole. In this section, we specialize to a universe where the inhomogeneities could be described as small perturbations on top of a flat FLRW background spacetime. We work in a conformal Newtonian gauge (our result is gauge invariant):

$$ds^2 = \bar{a}^2[-[1 + 2\Phi]d\eta^2 + ([1 - 2\Phi]\delta_{ij})], \quad (103)$$

where  $\delta_{ij}$  is the metric of the Minkowski spacetime,  $\bar{a}$  is the scale factor of the expanding background FLRW

spacetime, and  $\Phi$  is the Newtonian gravitational potential. The components of the timelike four velocity in perturbation theory are given by

$$u^0 = 1 - \Phi + \frac{3}{2}\Phi^2 - \frac{1}{2}\Phi^{(2)} + \frac{1}{2}\partial_i v \partial^i v, \quad (104)$$

$$u^i = \partial^i v + \frac{1}{2}v^{i(2)} + \frac{1}{2}\partial^i v^{(2)}, \quad (105)$$

where  $v^i$  is the peculiar velocity,  $\partial_i$  is the spatial derivative on the Minkowski spacetime in Cartesian coordinates, and  $v$  is the peculiar velocity potential. The indices with the small English alphabets denote the spatial component of the spacetime. The green superscripts denote terms evaluated at second order in perturbation theory.

Using Eqs. (103), (104), and (105) at leading order in perturbation theory, the shear tensor,  $\sigma^{ab}$  becomes

$$\sigma_{ij}(\eta, \mathbf{x}) = \bar{a}\partial_{(i}\partial_{j)}v(\eta, \mathbf{x}). \quad (106)$$

The ensemble average of the shear scalar is given

$$\frac{\sigma_{ab}\sigma^{ab}}{H^2} = \frac{2}{3}f^2(z)\sigma_R^2(z), \quad (107)$$

where  $f$  is the rate of growth of structures. We made use of the continuity to express the velocity potential and the in terms of the matter density contrast  $\delta_m$

$$v(\mathbf{k}, \eta) = \frac{\mathcal{H}}{k^2}f(\eta)\delta_m(\mathbf{k}, \eta). \quad (108)$$

In addition, we introduced the variance in matter density field

$$\sigma_R^2 = \int_0^{k_{UV}} \frac{dk}{2\pi^2} [k^2 P_m(k)] = \int_0^\infty \frac{dk}{2\pi^2} [(kW(kR))^2 P_m(k)]. \quad (109)$$

Here,  $P_m$  is the power spectrum of the matter density field. We have introduced a top-hat window function,  $W$ , instead of a UV dependent momentum integral. The scale,  $R$ , will be fixed shortly. For the different determinations of the Hubble rate, we focused on the dominant terms only, perturbing the monopole of various definitions of the Hubble rate give

$$H_0^\mu = H_0^{\mu_i} \simeq \bar{H}_0, \quad (110)$$

$$H_0^{d_A} = H_0^{d_L} = H_0^{\alpha_{||}} \simeq \bar{H}_0 \left[ 1 - \frac{4}{45}f^2(z)\sigma_R^2(z) \Big|_0 \right]. \quad (111)$$

Note that  $\Theta$  is well described by the FLRW background spacetime to an accuracy better than 0.1% [84], thus we neglect its perturbations and approximate  $H_0^\mu$  and  $H_0^{\mu_i}$  with

the FLRW background prediction,  $\bar{H}_0$ . The relationship between the rest of Hubble rate determinations and  $H_0^{\mu_i}$  is given

$$\frac{H_0^{\alpha_{||}}}{H_0^{\mu_i}} = 1 - \frac{4}{45}f^2(z)\sigma_R^2(z) \Big|_0. \quad (112)$$

Therefore, the BAO determination of the Hubble rate differs from the local measurements by a factor of  $1 - 4f^2(0)\sigma_R^2/45$ . The electric part of the Weyl tensor,  $E_{ab}$ , at leading order in perturbation theory is given by

$$E_{ij}(\eta, \mathbf{x}) = \partial_{(i}\partial_{j)}\Phi(\eta, \mathbf{x}). \quad (113)$$

We use the Poisson equation to express  $\Phi$  in terms  $\delta_m$

$$\Phi(\mathbf{k}, \eta) = -\frac{3}{2}\Omega_m(z) \left( \frac{\mathcal{H}}{k} \right)^2 \delta_m(\mathbf{k}, \eta), \quad (114)$$

where  $\Omega_m$  is the matter-energy density parameter. Using Eqs. (108) and (114) we find that

$$\frac{\sigma^{ab}E_{ab}}{H^3} = -\Omega_m f(z)\sigma_R^2(z). \quad (115)$$

Expanding the first two terms in  $q_0 = (\frac{1}{6}\rho - \frac{1}{3}\Lambda + \sigma^{ab}\sigma_{ab})/H_0^2$  up to second order in perturbation theory gives

$$\begin{aligned} \frac{1}{H_0^2} \left( \frac{11}{6\rho} - \frac{1}{3}\Lambda \right) \Big|_{z_0} &\approx \bar{q}_0 - \frac{1}{3H_0}\Omega_m\delta_m\partial^2v \\ &+ \frac{1}{3H_0^2}\bar{q}_0(\partial^2v)^2, \end{aligned} \quad (116)$$

$$\approx \bar{q}_0 + \frac{1}{3}\Omega_m f(0)\sigma_R^2 + \frac{1}{3}\bar{q}_0 f^2(0)\sigma_R^2. \quad (117)$$

The product of  $q_0$  and shear scalar in perturbation theory is given by

$$\frac{1}{H_0^2} \left( \frac{11}{6\rho} - \frac{1}{3}\Lambda \right) \Big|_{z_0} \frac{\sigma_{ab}\sigma^{ab}}{H^2} \Big|_{z_0} = \frac{2}{3}\bar{q}_0 f^2(0)\sigma_R^2, \quad (118)$$

where  $\bar{q}_0$  is the deceleration parameter on the background FLRW spacetime with the dust and cosmological constant

$$\bar{q}_0 = \frac{\Omega_m}{2} - \Omega_\Lambda = -1 + \frac{3}{2}\Omega_m, \quad (119)$$

where  $\Omega_\Lambda$  is the energy density due to the cosmological constant. In the second equality, we made use of the Friedmann equation  $\Omega_m + \Omega_\Lambda = 1$  to express  $\bar{q}_0$  in terms of  $\Omega_m$  only. The matter density and the cosmological constant today are defined in terms of these parameters

as  $\bar{\rho}_0 = 3\mathcal{H}_0^2\Omega_{m0}$  and  $\Lambda = 3\mathcal{H}_0^2\Omega_{\Lambda 0}$ . Using Eq. (117),  $q_0$  perturbed up to second order is given by

$$\begin{aligned} & \frac{1}{H_0^2} \left( \frac{1}{6}\rho - \frac{1}{3}\Lambda + \sigma^{ab}\sigma_{ab} \right) \\ & \simeq \bar{q}_0 + \frac{1}{3}\Omega_m f(0)\sigma_R^2 + \frac{1}{3}\bar{q}_0 f^2(0)\sigma_R^2 + \frac{2}{3}(f^2(0))\sigma_R^2(z). \end{aligned} \quad (120)$$

Finally, the deceleration parameter for both cases becomes

$$q_0^{d_A} = q_0^{d_L} \simeq \bar{q}_0 + \frac{11}{15}\Omega_m f(0)\sigma_R^2 + \left( \frac{7}{9}\bar{q}_0 + \frac{2}{5} \right) f^2(0)\sigma_R^2, \quad (121)$$

$$q_0^\mu = q_0^{\mu'} \simeq \bar{q}_0 + \frac{3}{5}\Omega_m f(0)\sigma_R^2 + \left( \frac{7}{9}\bar{q}_0 + \frac{2}{5} \right) f^2(0)\sigma_R^2. \quad (122)$$

The exact magnitude of the difference between the predictions of the effective Hubble rate and deceleration parameter from different ways of fitting an FLRW model to a lumpy universe depends on  $\sigma_R^2$ . We discuss how we handle the dependence on  $\sigma_R^2$  in Sec. IV A.

### A. Causal horizon and the expanding regions of spacetime

In cosmology, the well-known causal limits are determined by the dynamics on the null cone, for example, the particle horizon, which indicates the maximum distance light from particles could have travelled to the observer in the age of the Universe. Ellis and Stoeger argued in [85] that there exists a causal horizon that is determined not by the dynamics on the light cone but by the dynamics of our timelike geodesic. It is given by the boundary of the comoving region that has contributed most significantly to the dynamics of our local environment. The dominant interaction within this region are not mediated by massless particles (i.e., the vector and tensor perturbations on an FLRW background spacetime have negligible impact on the dynamics within this region); instead, they are mediated by massive particles that travel at very low speeds relative to the cosmic rest frame. It is these differences in speed that cause our local environment to decouple from the Hubble expansion because it cannot keep up the cosmic rest frame [85,86]. We determine the causal horizon as the comoving radius where divergence of our four velocity vanish. This is also called the zero-velocity surface [87]. At the leading order in cosmological perturbation theory, this is given by

$$\Theta \simeq 3H_0 + \partial_i \partial^i v|_{z=0} = 3H_0 + \frac{c}{r} \frac{d \ln \rho}{d \ln r}. \quad (123)$$

In the second equality, we made use of the continuity equation:  $\delta'_m = -\partial_i \partial^i v$  with  $\delta_m \equiv \delta\rho/\bar{\rho} = (\rho - \bar{\rho})/\bar{\rho}$  and use the chain rule to express the conformal time derivative of  $\delta_m$  in terms of radial derivative of  $\rho$

$$\delta'_m = \frac{d\delta_m}{d\eta} = \frac{1}{\bar{\rho}} \frac{\partial r}{\partial \eta} \frac{\partial \rho}{\partial r} \approx -\frac{1}{\bar{\rho}} \frac{\partial \rho}{\partial r} \approx -\frac{c}{r} \frac{d \ln \rho}{d \ln r}. \quad (124)$$

The radius of the zero-velocity surface  $\Theta(0, r) = 0$  is given by

$$R_0 = -\frac{c}{3H_0} \frac{d \ln \rho}{d \ln r}. \quad (125)$$

The spacetime in the region  $r < R_0$  are not expanding and it defines the local sphere of influence with respect to the observer. We estimate Eq. (123) using a dark matter halo model with the Einasto [88] and Navarro—Frenk—White (NFW) profiles [89] with the outer profile given by the mean matter density [90]. The result is shown in Fig. 1.  $R_0$  is obtained from Fig. 1 as the value of  $r$  where the curves intersect the  $\Theta(0, r) = 0$  horizontal line. We find that  $R_0$  is dependent on the mass of the host halo. The larger the halo mass, the higher the causal horizon. One might ask, how is  $R_0$  related to the virial radius,  $r_{\Delta_c}$  ( $\Delta_c$  is an overdensity constant). The mass contained with  $r_{\Delta_c}$  (virial mass) is the mass of a gravitationally bound astrophysical system, assuming the virial theorem holds. Recent studies have shown that  $r_{\Delta_c}$  does not correspond to the physical boundary of a gravitationally bound astrophysical system. The reason is that the mass contained within  $r_{\Delta_c}$  is subject to pseudoevolution [91,92]. And there are physical processes that are known to redistribute substructures formed during collapse from small to large radii greater than  $r_{\Delta_c}$  [93–95]. For these reasons, the splashback radius,  $r_{\text{sp}}$ , was introduced as a radius that includes all matter that orbits a halo [91,96]. The splashback radius of haloes of different masses is shown in the right panel of Fig. 1. We find that  $R_0$  is different from the splashback radius of the host halo. In fact from Fig. 1, we find that  $R_0$  is always greater than the  $r_{\text{sp}}$  at any of the given halo mass we considered. There are observational constraints for the radius of the zero-velocity surface for our local group  $R_0 \sim (0.95\text{--}1.05)$  Mpc [30,87,97] and this is the value we use for the rest of the analysis.

### B. The cosmological tensions: Hubble rate, absolute magnitude and the deceleration parameter

Now that we have determined the minimum length scale participating in the cosmic expansion, it is straightforward to calculate the Hubble discrepant [i.e., Eq. (112)]. The minimum length scale corresponds to the distance where the reference flux or the absolute magnitudes of sources in the Hubble flow are calibrated. This makes sense because cosmic evolutionary effect does not contribute to the absolute magnitude. Setting the smoothing scale to the

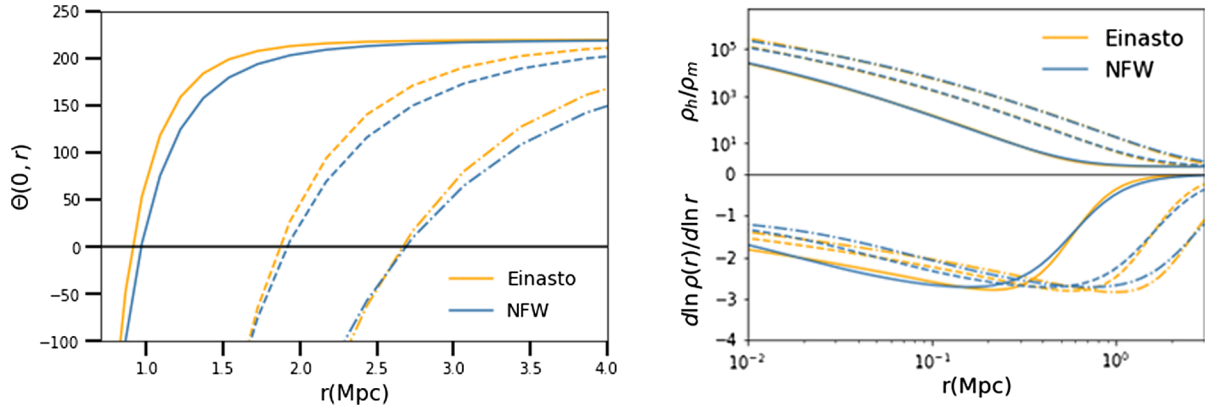


FIG. 1. The horizontal line in the left panel shows the zero-velocity (expansion) surface:  $\Theta(0, R\hat{n}) = 0$ , i.e., the transition radius where the spacetime goes from expansion to contraction. The exact position of  $R$  depends on the halo mass. The three curves, thick, dashed, and dash-dotted lines, correspond to the following halo masses  $M = [10^{11}, 10^{12}, 10^{13}] M_{\odot}$ , respectively. On the right panel, we compute the gradient of the halo density only for the same halo masses shown in the left panel. The splashback radius for a given halo mass is the position of the least gradient. The splashback radius is always less than the radius of the zero-velocity surface. In both cases, we fixed the halo concentration at 5.

radius of the zero-velocity surface  $R = R_0$ . The full result is shown in Fig. 2. We find about  $\sim(9\text{--}12)\%$  difference in the determination of the Hubble rate between the local measurements using the cosmic distance ladder and the BAO determinations.

Although, the cosmological interpretation of the peak magnitude of the SNIa by the SHOES and CCHP groups was done using a smooth luminosity distance, Both groups differ on the calibration of the supernova absolute magnitude. The SHOES build a local cosmic distance ladder using distance measurements to a set of anchors to infer the absolute magnitude of the SNIa. Other than using the standard formula for the parallax for the Milky Way Cepheids or the inverse square law for flux for the detached eclipsing binaries, or Leavitt’s law for Cepheids [98], etc.,

the process of calibrating the absolute magnitude of the SNIa is cosmological model independent. Since these sets of anchors live nearby, the calibration of the local cosmic distance ladder includes the impact of the tidal deformations on the local spacetime that we discuss here [35]. We showed how the impact of the tidal deformation results in a renormalization of the absolute magnitude in Sec. III B. Calibrating the SNIa absolute magnitude using the proper distance acoustic waves could have travelled from the origin of the Universe to the surface of the last scattering as an anchor, requires that we assume a particular model based on the FLRW spacetime. This model does not include the impact of the tidal field on distance measurement [82].

The supernova absolute magnitude tension refers to the disparity in the determination of the supernova absolute

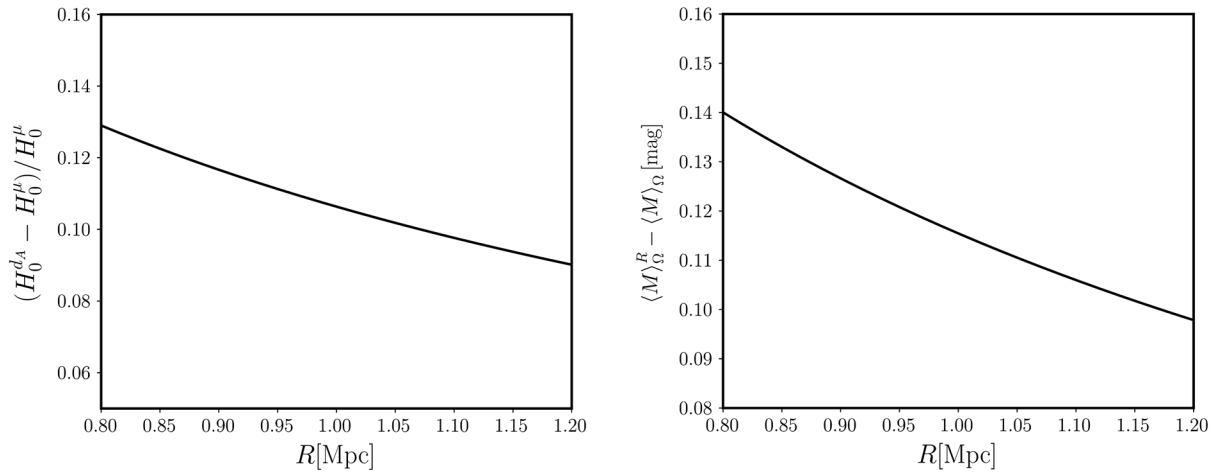


FIG. 2. Left panel: we show the fractional difference between the Hubble rates determined using the local measurement of the peak apparent magnitude of SNIa and the interpretation of the Alcock-Paczyński parameters in terms of the FLRW spacetime. Right panel: we show the difference between the renormalized absolute magnitude due to the impact of the tidal deformations on the distance to the anchor and the intrinsic absolute magnitude. We made use of the linear theory matter power spectrum to evaluate these.

magnitude between the inverse distance ladder method with the sound horizon scale at the surface of the last scattering as an anchor and local cosmic distance ladder with the anchors in the nearby universe [83,99]. Using the inverse distance method on Pantheon supernova peak magnitudes, [33] found the absolute magnitude to be

$$M^{\text{P18}} = -19.387 \pm 0.021 \text{ mag.} \quad (126)$$

For this same supernova sample, but using the SHOES Cepheid photometry for the geometric distance estimates, [33] finds the absolute magnitude to be

$$M^{\text{E21}} = -19.214 \pm 0.037 \text{ mag.} \quad (127)$$

The difference between Eqs. (126) and (127) is given by

$$M^{\text{E21}} - M^{\text{P18}} = 0.173 \pm 0.04 \text{ mag.} \quad (128)$$

We can relate Eq. (126) to  $\langle M \rangle_{\Omega}$  and Eq. (127) to  $\langle M \rangle_{\Omega}^R$  so that the difference between them is given by Eq. (76)

$$\langle M \rangle_{\Omega}^R - \langle M \rangle_{\Omega} = \frac{2}{9 \log 10} f^2(0) \sigma_R^2. \quad (129)$$

We show the result of calculating Eq. (129) in the right panel of Fig. 2. With  $R = D = 1$  Mpc, we find a difference of about 0.12 mag

In addition to the Hubble rate and the absolute magnitude, we also derived the expression for the deceleration parameter by fitting the FLRW model to the monopole of an inhomogeneous model of the area distance, distance modulus, etc. In this case, we find that both the local measurements and the BAO measurements (Alcock-Paczyński parameters) give deceleration parameter that differ substantially from the prediction of an FLRW model

$$q_0^{d_A/\mu} - \bar{q}_0 = \Delta q_0^{d_A/\mu}, \quad (130)$$

where  $\Delta q_0^{d_A/\mu}$  depends on the scalar invariant of a combination of shear tensor and the electric part of the Weyl tensor, i.e.,  $\sigma^{(ab)} E_{(ab)}/H^2|_{z=0}$  and  $\sigma_{ab} \sigma^{ab}/H^2|_{z=0}$ . The corresponding cosmological perturbation limit of both expressions are given in Eqs. (121) and (122). Again the local cosmic ladder and the Alcock-Paczyński parameter determinations of the deceleration parameter differ only in the coefficient of this term  $\sigma^{(ab)} E_{(ab)}/H^2|_{z=0}$  [see Eq. (101)].  $\sigma^{(ab)} E_{(ab)}/H^2|_{z=0}$  is related to the spatial curvature of the local domain.

We show in Fig. 3, the fractional difference between the deceleration parameters derived in Eqs. (121) and (122) and the FLRW predictions. We found over a 100% difference between the deceleration parameter from the local measurement interpreted based on an FLRW model and

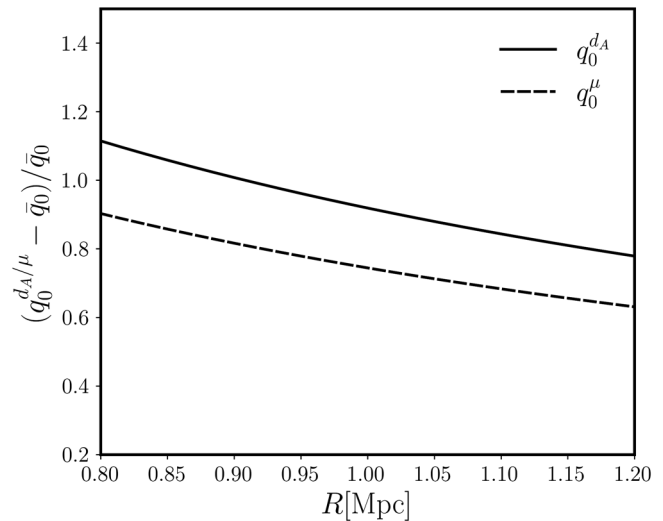


FIG. 3. We show the fractional difference between the deceleration parameters derived in Eqs. (121) (thick lines) and (122) (dashed lines) and the FLRW predictions.

Planck prediction. This finding is consistent with the recent measurements of the deceleration parameter using the Pantheon supernova samples and the cosmographical expression for the luminosity distance in FLRW limit [34,99]. However, it differs from the measurement of the deceleration parameter by the SHOES collaboration [36]. Note that the SHOES collaboration made use of the full expression for the luminosity distance based on the background FLRW spacetime and not its cosmographical approximation [79]. Given that [36] made use of the dataset used by [34,99] but supplemented with another dataset that is composed of high redshift SNIa. It is most likely that the reason for this disparity is related to the breakdown of Taylor series expansion in the presence of structures as reported in [35].

The Hubble tension is usually described as a discrepancy between the early and late-time Universe determination of the Hubble rate [21]. We have shown that it could be a consequence of how the distance measurements in the neighborhood of the observer are interpreted within the  $\Lambda$ CDM model. The key factor is that the local spacetime around the observer is tidally deformed, the background FLRW spacetime does not capture this effect. We showed that the model of area/luminosity distance that includes the effects of inhomogeneities through the perturbation of the FLRW spacetime would be able to explain the Hubble tension without any need of invoking any exotic evolving dark energy [100,101] (see Refs. [102,103] for a list of all possible models within this framework), frame-dependent dark energy [104] (this approach explains the SHOES result but gives a large value of the Hubble constant from the BAO analysis), quantum measurement uncertainties [105], evolving gravitational constant [106], modification of gravity [107,108]. One unique thing about all these approaches except the frame dependent dark energy which

breaks 4D diffeomorphism invariance but retains 3D coordinate invariance is that they assume that the FLRW background spacetime is valid on all scales and at all times. This is contrary to the findings in [35] that showed that the FLRW background spacetime in the presence of structures break down at about 1 Mpc. This scale is consistent with the scale where caustics or conjugate points appears [109]. Appearance of the conjugate points is a unique indicator for the breakdown of the coordinate system [29].

Furthermore, we showed that the interpretation of the BAO measurement (i.e., Alcock-Paczyński parameters) using the area distance based on the background FLRW spacetime infers a wrong  $H_0$  because the symmetries of background FLRW spacetime does not allow the contribution of the electric part of the Weyl tensor or the effect of the tidal deformations around the observer. If the Alcock-Paczyński parameters are consistently interpreted or evolved from high redshift to low redshifts using a model of the area distance that includes the impact of the tidal field or the area distance derived from a perturbed FLRW spacetime as described in [35], then the tensions in the Hubble parameter would not arise.

Of course, we are not the first to claim that the effects of inhomogeneities could resolve the Hubble tension. In fact it was argued in [110] that the large scale outflows due to the presence of local voids could be the cause of the Hubble tension and it could potentially explain the late time cosmic acceleration by dark energy [111]. The authors defined a spatial averaging procedure following the Buchert averaging formalism [112]. They found that an average under density of about  $\langle \delta \rangle = -0.3$  is enough to explain the discrepant Hubble rate. A more detailed study of this has shown that this does work [113]. Second, the authors did not compute the average values of what is observed; rather, they calculated the average density on the spatial hypersurface. An observer does not have access to the entire hypersurface; rather, it has access only to the screen space (2D surface) due to restriction imposed by the constant speed of light [114]. Similarly, it has been conjectured that anisotropies in the superhorizon perturbations could explain the Hubble tension. This approach has some fine-tuning issues to resolve. This simplest model of this has three free parameters that have to be chosen precisely for it to work [115].

## V. CONCLUSION

We have deployed the cosmological fitting approach introduced by Ellis and Stoeger [7,44] to study how well the FLRW spacetime fits an inhomogeneous universe on average. The FLRW model could be characterized by a set of free parameters such as the Hubble rate, deceleration parameter, etc., and we show how to obtain the best-fit Hubble rate and the deceleration parameter given generalized inhomogeneous models of the following observables: Alcock-Paczyński parameters, magnitude-redshift relation, and the intercept of the distance modules.

We made use of the results of the low redshifts Taylor series expansion of the generalized inhomogeneous expression of the area distance and luminosity distance developed by Kristian and Sachs in 1966 [24]. Using the 1 + 3 covariant decomposition formalism, we decomposed these expressions in terms of irreducible observables with respect to a geodesic observer. In this limit, the only key observables are the rate of expansion (a scalar) and the rate of shear deformation tensor. The rate of expansion scalar describes the rate at which nearby geodesics expands/contract with respect to a geodesic observer. It corresponds to the Hubble rate in the FLRW limit. The shear tensor, on the other hand, describes the rate of change of the spacetime deformation in the neighborhood of the observer [26]. It vanishes in the FLRW limit.

Using these tools, we derived the generalized inhomogeneous equations for the Alcock-Paczyński parameters. The Alcock-Paczyński parameters constrain the imprints of the Baryon Acoustic Oscillation in the galaxy distribution through the  $N$ -point correlation function. These parameters are usually interpreted in terms of the background FLRW model. We showed how to generalize the two components of the Alcock-Paczyński parameters to an inhomogeneous spacetime model. By comparing the monopole of the generalized radial component to the corresponding FLRW counterpart, we find that the inferred Hubble rate is biased by the impact of the tidal deformation tensor at the observer location. The orthogonal part is proportional to the area distance, hence we compare the monopole of the generalized area distance to the corresponding FLRW limit. At the leading order in redshift, we find that the Hubble rate today is biased as well by the scalar invariant of the shear tensor. At second order in redshift, we obtain the generalized expression for the deceleration parameter, which is also biased by the scalar invariant of the shear tensor and the product of the shear tensor and the electric part of the Weyl tensor.

Furthermore, we considered the magnitude-redshift relation. This is the key observable from which the determination of the Hubble rate is made from the peak magnitude of the type IA supernovae. We showed that the tidal deformation tensor that biases the determination of the Hubble rate from the monopole of the Alcock-Paczyński parameters impacts the measurement of the supernova absolute magnitude instead. The Hubble rate, in this case, is not biased, it corresponds exactly to the rate of expansion scalar which describes the rate of volume expansion/contraction. The deceleration parameter, however, is biased by the same terms as in the case of the orthogonal component of the Alcock-Paczyński parameter.

We quantified these terms within the cosmological perturbation theory assuming Gaussian and adiabatic initial conditions. We showed that the expectation value of these biasing terms is proportional to the smoothing scale-dependent variance in the matter density field. We argued that the most physically motivated smoothing scale corresponds to the comoving radius (causal horizon) where

the spacetime region goes from a contracting to an expanding phase. We use the halo model to quantify this exactly. We find that it is slightly greater than the splash-back radius of the host halo. Setting the mass of our local group to about  $\sim(10^{11}\text{--}10^{12}) M_\odot$ , we find the smoothing scale in the range of  $R \sim (0.8\text{--}1.2)$  Mpc. This leads to about  $\sim(8\text{--}12)\%$  fractional difference in the determination of the Hubble rate between the local measurements and the Alcock-Paczyński parameters. With the same range of values for the smoothing scales, we find that it explains the supernova absolute magnitude tension [33,99] and the values obtained from recent measurement of the deceleration parameter today using the Pantheon supernova samples [34]. The interpretation of the inferred values of the deceleration parameters should be taken with caution because cosmography in the presence of structures at second order in redshift differs from the full expression by more than 100% at about  $z \sim 0.1$ .

Finally, it is undeniable that the FLRW spacetime has played a big role in our current understanding of the Universe. Our results show that the tidal deformation of the observer spacetime region due to the gravitational interaction among nearby structures cannot be neglected. This interaction is characterized by tensors that vanish on the FLRW background spacetime. We have shown that not taking these into account when using the FLRW model alone to analyze cosmological observation leads to cosmological tensions. We showed that the determination of Hubble rate from the analysis of the local distance ladder for the SNIa peak magnitudes takes into account the impact of the tidal deformation of the local spacetime consistently.

### ACKNOWLEDGMENTS

I benefited immensely from discussions with Chris Clarkson, Robert Crittenden, Pierre Fleury, Emir Gumrukcuoglu, Asta Heinesen, Mathew Hull, Antony Lewis, Kazuya Koyama, and Daniela Saadeh. The works by G. F. R. Ellis on this topic have been very influential. O. U. is supported by the UK Science & Technology Facilities Council (STFC) Consolidated Grants Grant No. ST/S000550/1 and the South African Square Kilometre Array Project. The perturbation theory computations in this paper were done with the help of tensor algebra software xPand [116], which is based on xPert [117]. I made use of COLOSSUS (a PYTHON toolkit for cosmology, large-scale structure, and dark matter halos) developed by Benedikt Diemer for computations involving the dark matter halo profiles [90]. No new data were generated or analyzed in support of this research.

### APPENDIX: COVARIANT COSMOGRAPHY ON THE PAST LIGHT CONE

The distance-redshift relation on arbitrary spacetime may be expanded in Taylor series up to any order following the

formalism developed by Kristain and Sachs [24]. The formalism uses the null focusing equation to propagate the deviation vector,  $\xi^a$ , with the tail on the central ray,  $L$  and head on the nearby geodesics from a source with four velocity  $u_s^a$  to the observer with four velocity  $u_o^a$

$$\frac{d^2 \xi^a}{d\lambda^2} = -R^a{}_{cbd} k^c k^d \xi^b, \quad (\text{A1})$$

where  $R^a{}_{cbd}$  is the Riemann curvature tensor,  $\xi^a$  lives on the screen space, and  $k^a$  is the tangent vector to the null geodesics. The solution to Eq. (A1) needs to satisfy the following initial conditions at source

$$\begin{aligned} (\xi^a)_s &= 0, & \left(\frac{d\xi^a}{d\lambda} u_a\right)_s &= 0, \\ \left(\frac{d\xi^a}{d\lambda} k_a\right)_s &= 0, & \pi\left(\frac{d\xi^a}{d\lambda} \frac{d\xi^a}{d\lambda}\right)_s &= -(u_a k^a)_s d\Omega. \end{aligned} \quad (\text{A2})$$

Equation (A1) is valid provided there are no focal points between the observer and the source. Expanding  $(\xi_a \xi_b)$  in Taylor series in  $\lambda$  up to fifth order, gives

$$\begin{aligned} (\xi_a \xi_b)_o &= (\xi_a \xi_b)_s + \left[\frac{d}{d\lambda} (\xi_a \xi_b)\right]_s \lambda_o + \frac{1}{2} \left[\frac{d^2}{d\lambda^2} (\xi_a \xi_b)\right]_s \lambda_o^2 \\ &+ \mathcal{O}(\lambda_o^3). \end{aligned} \quad (\text{A3})$$

Using Eq. (A1) and the boundary conditions [Eq. (A2)] gives

$$(\xi_a \xi_b)_o = \lambda_o^2 \left(\frac{d\xi^c}{d\lambda} \frac{d\xi_c}{d\lambda}\right)_s \left(g_{ab} - \frac{1}{3} k^c k^d R_{acbd} \lambda_o^2 + \mathcal{O}(\lambda_o^3)\right). \quad (\text{A4})$$

The area element is defined as  $dA = \sqrt{(\xi_a \xi_b)_o} d\Omega$ , therefore

$$dA_o = d\Omega \lambda_o^2 (u_a k^a)_s^2 \left(1 - \frac{1}{6} k^c k^j R_{cj} \lambda_o^2 + \mathcal{O}(\lambda_o^3)\right). \quad (\text{A5})$$

To make contact with observation we expand the redshift in  $\lambda$

$$\begin{aligned} (1+z) &= \frac{E_s}{E_o} = \frac{1}{(k^a u_a)_o} \left[ k^a u_a + k^a k^b \nabla_a u_b \lambda \right. \\ &\left. + \frac{1}{2} k^a k^b k^c \nabla_a \nabla_b u_c \lambda^2 + \mathcal{O}(\lambda^3) \right]. \end{aligned} \quad (\text{A6})$$

Using the fact that the area distance is the ratio of the cross sectional area at the observer to the cross sectional area at the source according to

$$d_A^2 = \frac{dA_o (u_a k^a)_o^2}{d\Omega (u_a k^a)_s^2}. \quad (\text{A7})$$

Using Eq. (A5) in (A7) we find

$$d_A^2 = (u_a k^a)_0^2 \lambda_0^2 \left\{ 1 - \frac{1}{6} k^c k^d R_{cd} \lambda_0^2 + \mathcal{O}(\lambda_0^3) \right\}. \quad (\text{A8})$$

Inverting the series in Eq. (A8) gives the affine parameter in terms of the area distance,

$$\lambda_0 = d_A \left[ 1 + \frac{1}{12} K^c K^d R_{cd} d_A^2 + \mathcal{O}(d_A^3) \right], \quad (\text{A9})$$

where we defined normalized photon tangent vector  $K^a := \frac{k^a}{(u_a k^a)_0} = -u^a + n^a$ . Then putting Eq. (A9) in (A6) gives

$$z = K^a K^b \nabla_a u_b|_o d_A + \frac{1}{2} (K^a K^b K^c \nabla_a \nabla_b u_c)|_o d_A^2 + \mathcal{O}(d_A^3). \quad (\text{A10})$$

Inverting Eq. (A10) gives the area distance in terms of the redshift

$$d_A = \frac{z}{K^c K^j \nabla_c u_j|_0} \left\{ 1 - \left[ \frac{1}{2} \frac{K^c K^j K^k \nabla_k \nabla_j u_c}{(K^c K^j \nabla_c u_c)^2} \right]_0 z + \mathcal{O}(z^2) \right\}. \quad (\text{A11})$$

Using the reciprocity theorem  $d_L = d_A(1+z)^2$ , we find the luminosity distance to be

$$d_L = \frac{z}{K^c K^j \nabla_j u_c|_0} \left\{ 1 + \frac{1}{2} \left[ 4 - \frac{K^c K^j K^k \nabla_k \nabla_j u_c}{(K^c K^j \nabla_c u_c)^2} \right]_0 z + \mathcal{O}(z^2) \right\}. \quad (\text{A12})$$

- 
- [1] V. J. Martinez, M.-J. Pons-Borderia, R. A. Moyeed, and M. J. Graham, *Mon. Not. R. Astron. Soc.* **298**, 1212 (1998).
- [2] D. W. Hogg, D. J. Eisenstein, M. R. Blanton, N. A. Bahcall, J. Brinkmann, J. E. Gunn, and D. P. Schneider, *Astrophys. J.* **624**, 54 (2005).
- [3] P. Ntelis, A. Ealet, S. Escoffier, J.-C. Hamilton, A. J. Hawken, J.-M. Le Goff, J. Rich, and A. Tilquin, *J. Cosmol. Astropart. Phys.* **12** (2018) 014.
- [4] H. Boehringer, G. Chon, and J. Truemper, *Astron. Astrophys.* **651**, A16 (2021).
- [5] A. Nastasi, R. Fassbender, H. Böhringer, R. Šuhada, P. Rosati, D. Pierini, M. Verdugo, J. S. Santos, A. D. Schwöpe, A. de Hoon, J. Kohnert, G. Lamer, M. Mühlegger, and H. Quintana, *Astron. Astrophys.* **532**, L6 (2011).
- [6] U. Chadayammuri, J. ZuHone, P. Nulsen, D. Nagai, S. Felix, F. Andrade-Santos, L. King, and H. Russell, *Mon. Not. R. Astron. Soc.* **509**, 1201 (2021).
- [7] G. F. R. Ellis and W. Stoeger, *Classical Quantum Gravity* **4**, 1697 (1987).
- [8] C. Clarkson, G. Ellis, J. Larena, and O. Umeh, *Rep. Prog. Phys.* **74**, 112901 (2011).
- [9] J. Larena, *Springer Proc. Phys.* **157**, 385 (2014).
- [10] R. Maartens, *Phil. Trans. R. Soc. A* **369**, 5115 (2011).
- [11] C. Clarkson, *C. R. Phys.* **13**, 682 (2012).
- [12] A. G. Riess *et al.*, *Astrophys. J.* **826**, 56 (2016).
- [13] G. Pietrzyński *et al.*, *Nature (London)* **567**, 200 (2019).
- [14] M. J. Reid, D. W. Pesce, and A. G. Riess, *Astrophys. J. Lett.* **886**, L27 (2019).
- [15] W. L. Freedman, B. F. Madore, D. Hatt, T. J. Hoyt, I. S. Jang, R. L. Beaton, C. R. Burns, M. G. Lee, A. J. Monson, J. R. Neeley, M. M. Phillips, J. A. Rich, and M. Seibert, *Astrophys. J.* **882**, 34 (2019).
- [16] G. S. Anand, R. B. Tully, L. Rizzi, A. G. Riess, and W. Yuan, *Astrophys. J.* **932**, 15 (2022).
- [17] C. Alcock and B. Paczynski, *Nature (London)* **281**, 358 (1979).
- [18] L. Anderson *et al.*, *Mon. Not. R. Astron. Soc.* **439**, 83 (2014).
- [19] S. Alam *et al.* (BOSS Collaboration), *Mon. Not. R. Astron. Soc.* **470**, 2617 (2017).
- [20] O. H. E. Philcox, M. M. Ivanov, M. Simonović, and M. Zaldarriaga, *J. Cosmol. Astropart. Phys.* **05** (2020) 032.
- [21] E. Di Valentino, O. Mena, S. Pan, L. Visinelli, W. Yang, A. Melchiorri, D. F. Mota, A. G. Riess, and J. Silk, *Classical Quantum Gravity* **38**, 153001 (2021).
- [22] N. Aghanim *et al.* (Planck Collaboration), *Astron. Astrophys.* **641**, A6 (2020).
- [23] A. C. Rosell *et al.* (DES Collaboration), *Mon. Not. R. Astron. Soc.* **509**, 778 (2021).
- [24] J. Kristian and R. K. Sachs, *Astrophys. J.* **143**, 379 (1966).
- [25] G. F. R. Ellis, *J. Math. Phys. (N.Y.)* **8**, 1171 (1967).
- [26] G. F. R. Ellis and H. van Elst, *NATO Adv. Study Inst. Ser. C, Math. Phys. Sci.* **541**, 1 (1999).
- [27] F. A. E. Pirani, Introduction to gravitational radiation theory (Notes by J. J. J. Marek and the Lecturer), in *Lectures on General Relativity* (Prentice-Hall, Inc., 1965), Vol. 1, pp. 249–373, <https://ui.adsabs.harvard.edu/abs/1965gere.book..249P>.
- [28] K. S. Thorne, *Rev. Mod. Phys.* **52**, 299 (1980).
- [29] E. Witten, *Rev. Mod. Phys.* **92**, 045004 (2020).
- [30] Y.-S. Li and S. D. M. White, *Mon. Not. R. Astron. Soc.* **384**, 1459 (2008).
- [31] E. Carlesi, Y. Hoffman, J. G. Sorce, and S. Gottlöber, *Mon. Not. R. Astron. Soc.* **465**, 4886 (2017).
- [32] Z.-Z. Li and J. Han, *Astrophys. J. Lett.* **915**, L18 (2021).

- [33] G. Efstathiou, *Mon. Not. R. Astron. Soc.* **505**, 3866 (2021).
- [34] D. Camarena and V. Marra, *Phys. Rev. Research* **2**, 013028 (2020).
- [35] O. Umeh, arXiv:2201.11089.
- [36] A. G. Riess *et al.*, arXiv:2112.04510.
- [37] D. J. Schwarz, Thoughts on the cosmological principle, in *Fundamental Interactions: A Memorial Volume for Wolfgang Kummer*, edited by Grumiller Daniel *et al.* (World Scientific Publishing Co. Pte. Ltd, Singapore, 2010), pp. 267–276.
- [38] S. Sugiyama *et al.*, *Phys. Rev. D* **105**, 123537 (2022).
- [39] C. Zhao *et al.*, *Mon. Not. R. Astron. Soc.* **511**, 5492 (2022).
- [40] M. L. McClure and C. Hellaby, *Phys. Rev. D* **78**, 044005 (2008).
- [41] C. Hellaby and A. H. A. Alfedeel, *Phys. Rev. D* **79**, 043501 (2009).
- [42] K. Bolejko, C. Hellaby, and A. H. A. Alfedeel, *J. Cosmol. Astropart. Phys.* **09** (2011) 011.
- [43] T. H.-C. Lu and C. Hellaby, *Classical Quantum Gravity* **24**, 4107 (2007).
- [44] G. F. R. Ellis, *Fundam. Theor. Phys.* **9**, 215 (1984).
- [45] V. Perlick, *Living Rev. Relativity* **7**, 9 (2010).
- [46] L. Rizzi, R. B. Tully, D. Makarov, L. Makarova, A. E. Dolphin, S. Sakai, and E. J. Shaya, *Astrophys. J.* **661**, 815 (2007).
- [47] A. W. Mann and K. von Braun, *Publ. Astron. Soc. Pac.* **127**, 102 (2015).
- [48] B. F. Madore, W. L. Freedman, and A. Lee, *Astrophys. J.* **926**, 153 (2022).
- [49] A. Heinesen, *J. Cosmol. Astropart. Phys.* **05** (2021) 008.
- [50] I. Etherington, London, Edinburgh, Dublin Philos. Mag. J. Sci. **15**, 761 (1933).
- [51] G. F. R. Ellis, *Proc. Int. Sch. Phys. Fermi* **47**, 104 (1971).
- [52] G. F. R. Ellis, *Gen. Relativ. Gravit.* **41**, 581 (2009).
- [53] E. R. Peterson *et al.*, arXiv:2110.03487.
- [54] R. A. Sussman, J. C. Hidalgo, I. Delgado Gaspar, and G. Germán, *Phys. Rev. D* **95**, 064033 (2017).
- [55] H. J. Macpherson and A. Heinesen, *Phys. Rev. D* **104**, 023525 (2021); **104**, 109901(E) (2021).
- [56] J. Ehlers, P. Geren, and R. K. Sachs, *J. Math. Phys. (N.Y.)* **9**, 1344 (1968).
- [57] J. Ehlers, *Gen. Relativ. Gravit.* **25**, 1225 (1993).
- [58] G. F. R. Ellis, M. Bruni, and J. Hwang, *Phys. Rev. D* **42**, 1035 (1990).
- [59] K. S. Thorne, *Mon. Not. R. Astron. Soc.* **194**, 439 (1981).
- [60] T. Gebbie and G. F. R. Ellis, *Ann. Phys. (N.Y.)* **282**, 285 (2000).
- [61] G. F. R. Ellis, D. R. Matravers, and R. Treciokas, *Ann. Phys. (N.Y.)* **150**, 455 (1983).
- [62] T. Gebbie and G. F. R. Ellis, *Ann. Phys. (Amsterdam)* **282**, 285 (2000).
- [63] A. J. M. Spencer, *Int. J. Eng. Sci.* **8**, 475 (1970).
- [64] K. Thorne, *Rev. Mod. Phys.* **52**, 299 (1980).
- [65] S. Liotta, *Solid State Electron.* **44**, 95 (2000).
- [66] J. P. Jaric, *Int. J. Eng. Sci.* **41**, 2123 (2003).
- [67] C. Clarkson and O. Umeh, *Classical Quantum Gravity* **28**, 164010 (2011).
- [68] O. Umeh, The influence of structure formation on the evolution of the universe, Ph.D. thesis, University of Cape Town, Faculty of Science, Department of Mathematics and Applied Mathematics, 2013.
- [69] S. Nadathur, P. M. Carter, W. J. Percival, H. A. Winther, and J. Bautista, *Phys. Rev. D* **100**, 023504 (2019).
- [70] F. Beutler *et al.* (BOSS Collaboration), *Mon. Not. R. Astron. Soc.* **444**, 3501 (2014).
- [71] O. Umeh, C. Clarkson, and R. Maartens, *Classical Quantum Gravity* **31**, 205001 (2014).
- [72] Y. Hoffman, O. Metuki, G. Yepes, S. Gottlöber, J. E. Forero-Romero, N. I. Libeskind, and A. Knebe, *Mon. Not. R. Astron. Soc.* **425**, 2049 (2012).
- [73] J. E. Forero-Romero, S. Contreras, and N. Padilla, *Mon. Not. R. Astron. Soc.* **443**, 1090 (2014).
- [74] M. A. H. MacCallum and G. F. R. Ellis, *Commun. Math. Phys.* **19**, 31 (1970).
- [75] W. L. Freedman, *Astrophys. J.* **919**, 16 (2021).
- [76] W. L. Freedman, B. F. Madore, T. Hoyt, I. S. Jang, R. Beaton, M. G. Lee, A. Monson, J. Neeley, and J. Rich, *Astrophys. J.* **891**, 57 (2020).
- [77] A. G. Riess *et al.*, *Astrophys. J.* **861**, 126 (2018).
- [78] A. G. Riess, S. Casertano, W. Yuan, L. Macri, J. Anderson, J. W. MacKenty, J. B. Bowers, K. I. Clubb, A. V. Filippenko, D. O. Jones, and B. E. Tucker, *Astrophys. J.* **855**, 136 (2018).
- [79] A. G. Riess *et al.*, *Astrophys. J.* **659**, 98 (2007).
- [80] A. G. Riess, S. Casertano, W. Yuan, L. M. Macri, and D. Scolnic, *Astrophys. J.* **876**, 85 (2019).
- [81] A. G. Riess, S. Casertano, W. Yuan, J. B. Bowers, L. Macri, J. C. Zinn, and D. Scolnic, *Astrophys. J. Lett.* **908**, L6 (2021).
- [82] E. Aubourg *et al.*, *Phys. Rev. D* **92**, 123516 (2015).
- [83] D. Camarena and V. Marra, *Mon. Not. R. Astron. Soc.* **495**, 2630 (2020).
- [84] O. Umeh, J. Larena, and C. Clarkson, *J. Cosmol. Astropart. Phys.* **03** (2011) 029.
- [85] G. F. R. Ellis and W. R. Stoeger, *Mon. Not. R. Astron. Soc.* **398**, 1527 (2009).
- [86] G. F. R. Ellis, *Found. Phys.* **50**, 1057 (2020).
- [87] I. D. Karachentsev, O. G. Kashibadze, D. I. Makarov, and R. B. Tully, *Mon. Not. R. Astron. Soc.* **393**, 1265 (2009).
- [88] J. Einasto and U. Haud, *Astron. Astrophys.* **223**, 89 (1989).
- [89] J. F. Navarro, C. S. Frenk, and S. D. M. White, *Astrophys. J.* **462**, 563 (1996).
- [90] B. Diemer, *Astrophys. J. Suppl. Ser.* **239**, 35 (2018).
- [91] S. More, B. Diemer, and A. Kravtsov, *Astrophys. J.* **810**, 36 (2015).
- [92] O. Umeh, R. Maartens, H. Padmanabhan, and S. Camera, *J. Cosmol. Astropart. Phys.* **06** (2021) 027.
- [93] S. Kazantzidis, A. R. Zentner, and A. V. Kravtsov, *Astrophys. J.* **641**, 647 (2006).
- [94] M. Valluri, I. M. Vass, S. Kazantzidis, A. V. Kravtsov, and C. L. Bohn, *Astrophys. J.* **658**, 731 (2007).
- [95] I. P. Carucci, M. Sparre, S. H. Hansen, and M. Joyce, *J. Cosmol. Astropart. Phys.* **06** (2014) 057.
- [96] B. Diemer and A. V. Kravtsov, *Astrophys. J.* **789**, 1 (2014).

- [97] S. van den Bergh, *Astron. Astrophys. Rev.* **9**, 273 (1999).
- [98] H. S. Leavitt and H. Shapley, *Ann. Harv. Coll. Obs.* **85**, 143 (1930).
- [99] D. Camarena and V. Marra, *Mon. Not. R. Astron. Soc.* **504**, 5164 (2021).
- [100] M. G. Dainotti, B. De Simone, T. Schiavone, G. Montani, E. Rinaldi, and G. Lambiase, *Astrophys. J.* **912**, 150 (2021).
- [101] F. Niedermann and M. S. Sloth, *Phys. Rev. D* **105**, 063509 (2022).
- [102] L. Knox and M. Millea, *Phys. Rev. D* **101**, 043533 (2020).
- [103] E. Abdalla *et al.*, *J. High Energy Astrophys.* **34**, 49 (2022).
- [104] S. L. Adler, *Phys. Rev. D* **100**, 123503 (2019).
- [105] S. Capozziello, M. Benetti, and A. D. A. M. Spallicci, *Found. Phys.* **50**, 893 (2020).
- [106] G. Benevento, J. A. Kable, G. E. Addison, and C. L. Bennett, [arXiv:2202.09356](https://arxiv.org/abs/2202.09356).
- [107] M. Zumalacarregui, *Phys. Rev. D* **102**, 023523 (2020).
- [108] M. G. Dainotti, B. De Simone, T. Schiavone, G. Montani, E. Rinaldi, G. Lambiase, M. Bogdan, and S. Ugale, *Galaxies* **10**, 24 (2022).
- [109] C. Pichon and F. Bernardeau, *Astron. Astrophys.* **343**, 663 (1999).
- [110] L. Lombriser, *Phys. Lett. B* **803**, 135303 (2020).
- [111] M. Kasai and T. Futamase, *Prog. Theor. Exp. Phys.* **2019**, 073E01 (2019).
- [112] T. Buchert, *Gen. Relativ. Gravit.* **32**, 105 (2000).
- [113] W. D. Kenworthy, D. Scolnic, and A. Riess, *Astrophys. J.* **875**, 145 (2019).
- [114] T. Buchert, H. van Elst, and A. Heinesen, [arXiv:2202.10798](https://arxiv.org/abs/2202.10798).
- [115] P. Tiwari, R. Kothari, and P. Jain, *Astrophys. J. Lett.* **924**, L36 (2022).
- [116] C. Pitrou, X. Roy, and O. Umeh, *Classical Quantum Gravity* **30**, 165002 (2013).
- [117] D. Brizuela, J. M. Martin-Garcia, and G. A. Mena Marugan, *Gen. Relativ. Gravit.* **41**, 2415 (2009).